

Migmatite from the Tekkali Area, Eastern Ghats, India: Chemical Investigation and P-T Estimation

YAMAMOTO Tetsuya

Department of Geoscience, Faculty of Science, Osaka City University,
Osaka 558-8585, Japan

Abstract

A migmatite with a mineral assemblage of garnet-orthopyroxene-biotite widely occurs around the Tekkali area in the Eastern Ghats Mobile Belt (EGMB), India. The lithology changes from stromatic metatexite to plutonic diatexite, and between them a migmatite with coarse-grained orthopyroxene-bearing leucosome vein occurs ("veined migmatite"). The veined migmatite and diatexite are analyzed in terms of mineral and bulk rock chemistry. The mesosome portion of the veined migmatite has an appearance of garnet (~Prp₂₅) -biotite gneiss and involves fine-grained orthopyroxene (~En₅₅; Opx 1) and garnet porphyroblast (~Prp₂₆) surrounded by the leucocratic patches. The Opx 1 and garnet porphyroblast are considered to have formed concomitantly by the melting reaction consuming biotite+plagioclase+quartz of the possible protolith, metagraywacke. Coarse-grained orthopyroxene in the leucosome of the veined migmatite and diatexite is characterized by the presence of exsolution lamellae and Fe-enrichment (En₄₃; Opx 2). Garnet concentrated along the boundary of the mesosome and the leucosome shows similar composition to that in the mesosome, while it is Fe-rich (~Prp₂₂) in the diatexite.

The mesosome of the veined migmatite is interpreted to have suffered from a melting event at high temperature (~760°C) and middle pressure (~6.3 kbar) conditions, under the effect of percolated aqueous fluid. The diatexite, with higher temperature (~880°C) was emplaced at ~7.5 kbar. Whole rock chemistry of the leucosome of the veined migmatite and the diatexite, characterized by high K, Ti, Ba and Sr, indicates that they are similar to Charnockitic Magma Type (CMT). The thermal event of the area is suggested as follows: the CMT emplacement provided heat and aqueous fluid to the metagraywacke roof by vein propagation, and the roof part suffered from incipient melting to form the veined migmatite.

Garnet coronas (~Prp₂₀) surrounding Opx 2 were produced during an isobaric cooling event (IBC), which ceased at ~660°C and ~5.5 kbar in the veined migmatite, and at ~690°C and ~6.2 kbar in the diatexite. The IBC trajectory is approximately comparable with those previously reported in the EGMB. In the present study area, the IBC is considered to have followed the CMT emplacement.

Key words: Geochemistry, Geothermobarometer, Partial melting, Aqueous fluid, CMT

Introduction

At granulite temperature conditions, especially >~850°C, the prominent constituents of the crust are effectively fertile to create melt or magma of granitic composition, as confirmed by experimental studies (e.g., Skjerlie and Johnston, 1993). It follows that many studies have shown the migmatite being a record of fluid-absent melting in the mid- to lower crust, where the availability of water is considered very limited (e.g., Dasgupta et al., 1992; Braun et al., 1996). On the other hand, the problem whether or not the neosome-formation process is related to melting and fluid is still debated, as seen in the studies of charnockite. It has been recognized that various processes of charnockitic neosome formation, which include fluid-absent melting, melting under the effect of CO₂-rich fluid, subsolidus dehydration and so on (e.g., Newton, 1992;

Zhao et al., 1997 and references therein). The neosome formation may not be *in situ* but represents injection of melt derived from an external magma (Jung et al., 1998). Whichever the process, the occurrence of felsic plutonic lithology within a gneissic rock has been tempting petrologists because it is suggestive of material transport and differentiation in the crust. The present study area, located in the Eastern Ghats Mobile Belt, one of the Proterozoic high-temperature granulite terrains of India, includes various lithologies of migmatite; their leucosome portions characteristically consist of charnockitic assemblages. The variety of the occurrence and distribution of the migmatites is considered to reflect the factors that constrain the process of their formation. The present study aims to reveal the nature of the migmatization which resulted from a thermal event relating to charnockitic magma activity, by virtue of geochemistry and P-T estimation.

Geology

The present study area is located in the northwestern part of the Eastern Ghats Mobile Belt (EGMB) which consists of Proterozoic granulites. Garnet-orthopyroxene-biotite migmatite (GOBM) is widely distributed from Tekkali town to south of Patapatnam, and is separated from other granulites, mainly garnet-sillimanite gneiss (Yamamoto et al. 1998). The GOBM is particularly well-exposed around Tekkali Town, where it is zoned by stromatic metatexite and veined migmatite through diatexite from north to south (Fig. 1). In places, leucogranite sills/dykes occur in the veined migmatite (Fig. 2A). The veined migmatite is with the leucosome veins cutting across the mesosome in a network-pattern (Fig. 2A)

or along the axial planes of a minor folds (Fig. 2B). The diatexite has a plutonic lithology, trapping some ghost-like mesosome (Fig. 2C). Other granulites in the area include orthopyroxene-biotite gneiss, two-pyroxene granulite and calc-silicate rock (Fig. 1B). In this article, the veined migmatite and the diatexite are focused on.

Petrography

The petrographic features of the mesosome and leucosome of the veined migmatite and the diatexite are listed in Table 1. Mineral abbreviations follow Kretz (1983).

The mesosome of the veined migmatite is like a garnet (1-1.5mm in diameter)-biotite gneiss, but heterogeneous due

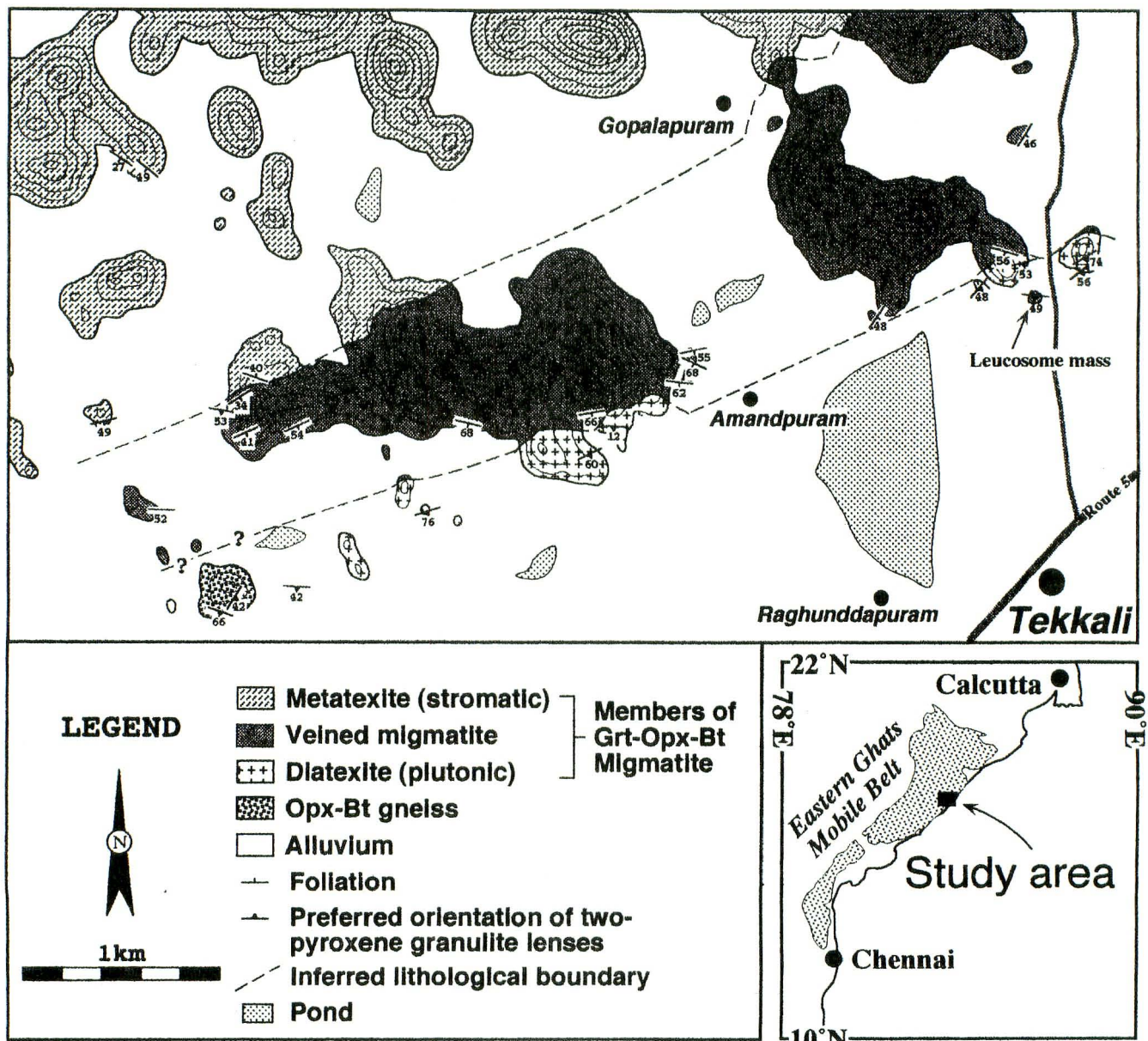


Fig. 1. Geological map of the Tekkali and its surrounding area. Inset shows the position of the study area in the Eastern Ghats Mobile Belt, India.

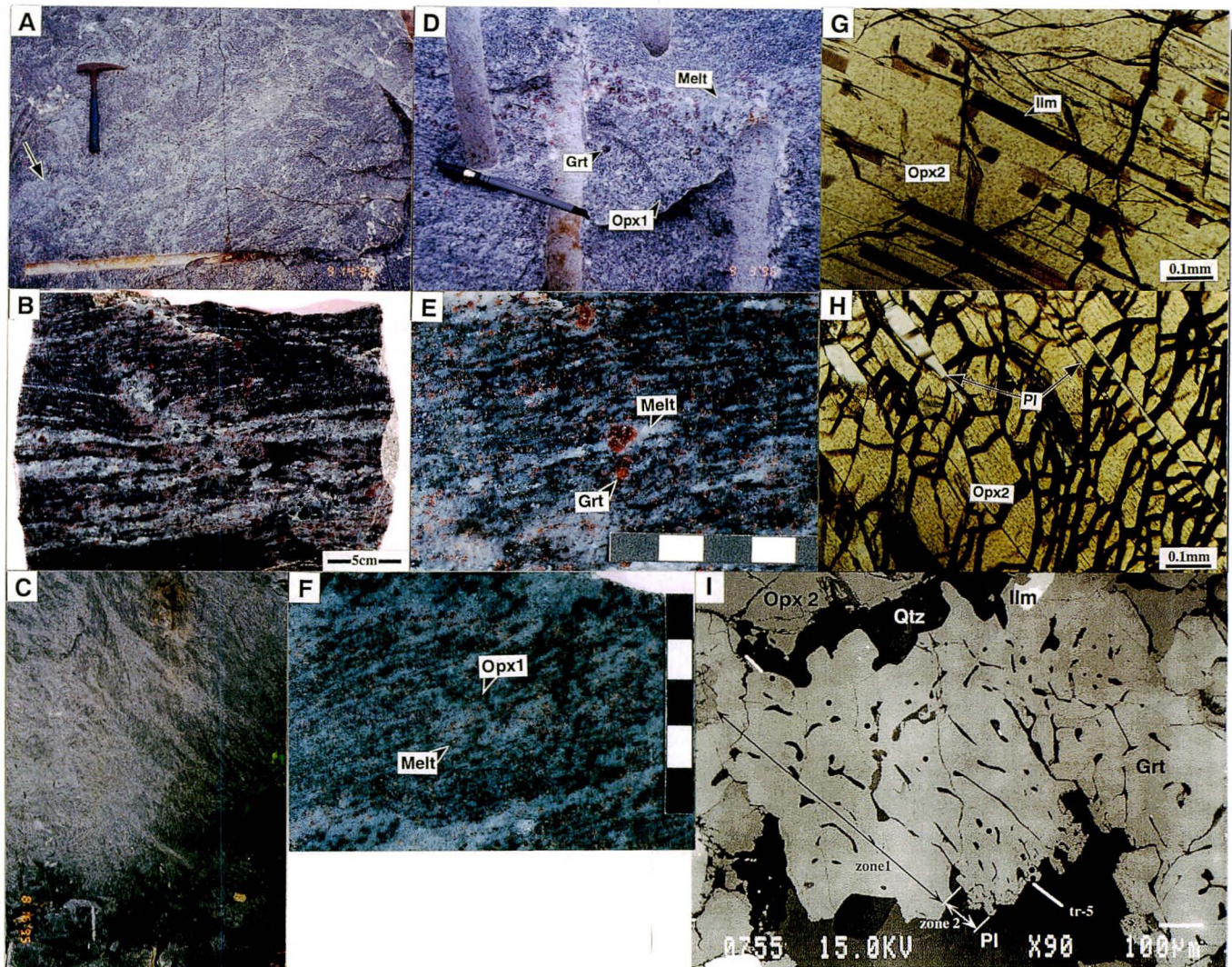


Fig. 2. A: Outcrop of the veined migmatite in which the leucosome veins develop network. Arrow indicates the leucogranite sill. B: Occurrence of the veined migmatite. Leucocratic portions in the mesosome parallel to the gneissosity retains initial melt. The coarse-grained orthopyroxene (Opx2)-bearing leucosome cut the mesosome along shear surface. C: Contact between the diatexite and the veined migmatite. D: Garnet porphyroblast surrounded by leucocratic pool constituting the melt remnant. E: Opx 1 within the leucocratic (melt) pool in the mesosome. F: Retrograde garnet formed between Opx 2 and plagioclase, with a traverse analyzed.

Table 1. Occurrences of mafic minerals and modal compositions of the GOBM. Numbers in brackets indicate diameter of garnet (mm), numbers of orthopyroxene is for Opx-types described in the text. +: present; R: retrograde phase; M: occurring as "melanosome"; G: generally forming gneissosity; I: occurring interstitially.

	Grt (1-1.5)	Grt (7)	R	Opx	Bt	Modal composition
Mesosome	+	+		1	G	granodiorite
Leucosome	M			+	2	I
Diatexite	+			+	2	I, R

to the presence of leucocratic portions with biotite rafts (Fig. 2B). The leucocratic portions are in the form of veins (2-3 mm in width), bands (< ~3 cm in width), parallel to the gneissosity, and patches. It is interpreted that the leucocratic portions have resulted from the melt, which percolated throughout the mesosome (Yamamoto et al., 1998). Garnet porphyroblast (~7 mm) and orthopyroxene (~0.5 mm; Opx 1) often occur in the leucocratic portions (Fig. 2D, E, F). Sub-euhedral, coarse- to medium-grained plagioclase having antiperthite lamella implies its growth from melt (e.g., Busch et al., 1974). Rounded quartz, plagioclase and biotite in garnet porphyroblast and Opx 1 are reactants that produced their host minerals and melt (Yamamoto et al., 1998). The garnet porphyroblast characteristically includes numerous acicular fluorapatites (~1.3 × 0.15 mm) and dusty inclusions (Niimi

and Yamamoto, 1998) distributed in a concentric circle. Flaky graphite is also rarely included.

The leucosome of the veined migmatite is characterized by coarse-grained orthopyroxene (Opx 2; < 50 mm in longer axis), which is preferentially distributed in the central portion of the leucosome (Fig. 2A, B). Crystallographically oriented ilmenite and plagioclase in the Opx 2 indicate their nature as exsolution lamellae (Fig. 2G, H) (e.g., Garrison and Taylor, 1981; Owens and Dymek, 1995). Opx 2 has inclusions or embayments of euhedral medium-grained plagioclase. Occurrence of biotite is rare and interstitial, and sometimes occurs as inclusions in feldspar. Euhedral garnet (1-1.5 mm) concentrates within 2-3 cm at the boundary between the leucosome and the mesosome ("melanosome"-like distribution) (Fig. 2B) and is similar to those in the mesosome. The petrography suggests a crystallizing order as: (Grt, Bt? trapped from the mesosome) Pl → Opx 2 → Kfs → Bt. A retrograde garnet rimming Opx 2 is texturally zoned. The inner zone 1 includes rod-shaped quartz, and the outer zone 2 includes finer quartz drops. The rim shape of zone 2 has euhedral facet (Fig. 2I).

The diatexite is petrographically similar to the leucosome, except that it has a little more garnet and biotite. The biotite is either interstitial, or in symplectitic texture with feldspars neighboring garnet. The garnet is considered to have been generated from the mesosome trapped in the diatexite, while symplectitic biotite indicates its formation by the reaction of garnet with melt. Ilmenite, pyrite, apatite and zircon occur in accessory amount in all the lithologies.

Analytical methods

Mineral compositions were analyzed using JEOL JXA-8600MX housed at Kochi University, except fluorine

bearing phases done at Osaka City University by Shimadzu EPMA-8705. An accelerating voltage of 15kv was maintained with a beam current of 15nA (JEOL) and 4nA (Shimadzu). The beam diameter was fixed at 1 μm . The oxide ZAF program supplied by JEOL was utilized for correction of counted values. For the F-bearing minerals, correction was done following Bence and Albee (1968).

Major and trace elements of whole rock were analyzed by XRF (RIGAKU RIX2000) at Fukuoka University of Education. The whole mineral composition of Opx 2 was done on Shimadzu VXQ-160S at Osaka City University. Current and voltage are fixed at 50kv and 50mA, respectively. The beam diameter was fixed at 30 mm. Sample glass bead was prepared from rock power diluted with dilithium tetraborate in the ratio 1:3. Sample powder of Opx 2 was prepared by hand-picking after mineral separation by Frantz L-1 isodynamic magnetic separator.

Mineral chemistry

Orthopyroxene: Opx 1 and 2 are En₅₃₋₅₇ and En₄₇₋₅₃ in the pyroxene quadrilateral, respectively, with a very little Wo component (CaO=0.21-0.43 wt%) (Fig. 3; Table. 2). Both orthopyroxenes are not zoned, but the Opx 2 is enriched in Mg (< 19.60 wt%) adjacent to retrograde garnet. Opx 1 is within the range of orthopyroxenes resulted from the melting experiments of metagraywacke (Fig. 4). Its extremely low Wo component is similar to the results by Montel and Vielzeuf (1997). The Al₂O₃ of orthopyroxenes in these experiments varies from ~2 to 13 wt%, while the Opx 1 has ~2 wt% of Al₂O₃, corresponding to a minimum amount within them.

The bulk analysis of the Opx 2 has higher FeO/MgO (En₄₃; Fig. 3), Al₂O₃, TiO₂ and CaO (Table. 2) than indicated by point-analysis; this is consistent with the presence of

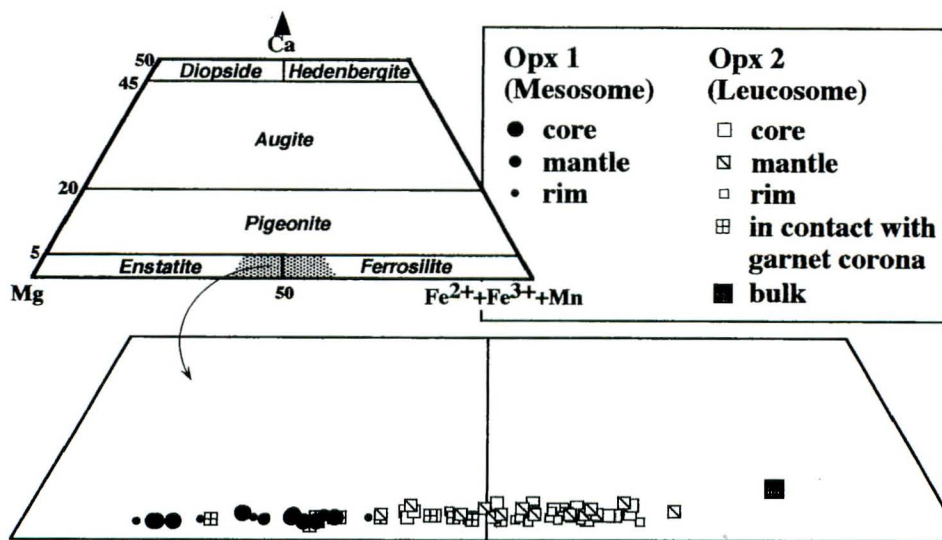


Fig. 3. Opx 1 and 2 plotted on the pyroxene quadrilateral. Pyroxene nomenclature after Morimoto et al. (1989).

Table. 2. Representative chemical analyseis of orthopyroxene. Formula unit normalized by O=6. c: core; m: mantle; r: rim for analytical positions. *: calculated. n.a.: not analized

RockType		Mesosome										Leucosome										Diatexite									
Sample		950804-1					950825-1					9610A					950822-1d														
Anal. No	b7	b10	b9	152	151	153	b11	b12	b13	b9.5	b11	b13-2	b23	81	79	80	120	e9	e8	e7	e11	e15	e17	Bulk							
Anal. Pos.	c	m	r	c	m	r	c	m	r	c	m	r	g	c	m	r	g	c	m	g	c	m	r	-							
SiO ₂	51.33	51.33	51.74	50.95	51.15	51.00	50.38	51.09	50.74	50.88	51.54	51.03	51.18	49.91	50.51	50.11	51.31	50.81	50.70	52.10	49.71	50.62	51.22	49.47							
TiO ₂	0.10	0.03	0.05	0.11	0.11	0.11	0.06	0.05	0.04	0.05	0.05	0.03	0.08	0.10	0.05	0.04	0.02	0.04	0.04	0.06	0.55	0.08	0.06	0.33							
Al ₂ O ₃	2.08	2.12	1.70	2.13	1.74	1.90	2.02	1.30	1.02	1.26	1.03	0.75	1.10	2.13	1.51	1.13	0.97	1.26	1.56	0.86	2.51	1.77	0.79	2.98							
Cr ₂ O ₃	0.00	0.00	0.03	0.03	0.00	0.00	0.00	0.03	0.05	0.02	0.03	0.02	0.02	0.01	0.04	0.00	0.01	0.04	0.00	0.00	0.004	0.00	0.02	n.a.							
*Fe ₂ O ₃	0.00	0.11	0.00	0.63	1.89	1.05	0.52	0.10	0.00	0.93	0.42	0.00	0.00	1.75	0.62	0.71	2.09	0.93	1.24	0.00	0.62	0.00	0.00	0							
FeO	26.99	27.35	26.57	27.76	27.14	26.61	30.13	29.71	31.58	28.53	28.81	30.80	30.24	30.43	30.03	26.97	30.46	30.05	26.78	30.75	31.34	31.55	31.78								
MnO	0.23	0.23	0.27	0.31	0.27	0.21	0.39	0.32	0.41	0.31	0.27	0.32	0.20	0.34	0.45	0.28	0.29	0.37	0.31	0.30	0.38	0.35	0.30	0.43							
MgO	18.81	18.76	19.23	18.31	18.78	19.03	16.44	17.24	15.79	17.72	18.06	16.54	17.99	16.18	16.39	16.47	18.89	16.52	16.68	19.20	15.96	15.98	16.19	14.12							
CaO	0.31	0.25	0.25	0.28	0.30	0.26	0.36	0.28	0.22	0.34	0.28	0.34	0.24	0.29	0.27	0.25	0.28	0.36	0.40	0.22	0.28	0.30	0.29	0.59							
Na ₂ O	0.00	0.01	0.00	0.00	0.00	0.01	0.00	0.00	0.01	0.00	0.00	0.00	0.00	0.00	0.00	0.00	0.07	0.02	0.01	0.02	0.00	0.00	0.03	0.25							
K ₂ O	0.00	0.00	0.00	0.00	0.00	0.00	0.00	0.00	0.00	0.00	0.00	0.00	0.00	0.00	0.00	0.00	0.02	0.01	0.00	0.01	0.01	0.04	0.03								
NiO	0.00	0.02	0.06	0.00	0.00	0.00	0.04	0.00	0.00	0.00	0.05	0.01	0.00	0.00	0.00	0.00	0.00	0.00	0.00	0.00	0.00	0.00	0.00	n.a.							
total	99.85	100.18	99.84	100.50	101.38	100.18	100.29	100.12	99.86	100.04	100.48	99.83	98.90	100.96	100.27	99.02	100.90	100.83	101.00	99.53	100.81	100.45	100.49	99.98							
Si	1.954	1.951	1.965	1.939	1.931	1.939	1.945	1.968	1.978	1.957	1.969	1.982	1.979	1.923	1.954	1.962	1.948	1.957	1.946	1.944	1.917	1.958	1.982	1.933							
Ti	0.003	0.001	0.001	0.003	0.003	0.003	0.002	0.001	0.001	0.001	0.001	0.001	0.002	0.003	0.001	0.001	0.001	0.001	0.001	0.004	0.016	0.002	0.002	0.010							
Al	0.093	0.095	0.076	0.096	0.078	0.085	0.092	0.059	0.047	0.057	0.046	0.034	0.050	0.097	0.069	0.052	0.044	0.057	0.071	0.085	0.114	0.081	0.036	0.137							
Cr	0.000	0.000	0.001	0.001	0.000	0.000	0.000	0.001	0.002	0.001	0.001	0.001	0.000	0.000	0.001	0.000	0.000	0.000	0.001	0.000	0.000	0.000	0.000								
Fe ³⁺	0.000	0.003	0.000	0.018	0.054	0.030	0.015	0.003	0.000	0.027	0.012	0.000	0.000	0.051	0.018	0.021	0.060	0.027	0.036	0.000	0.018	0.000	0.000	0.000							
Fe ²⁺	0.859	0.869	0.844	0.884	0.857	0.846	0.973	0.957	1.029	0.917	0.920	1.000	0.908	0.974	0.984	0.983	0.855	0.981	0.964	0.854	0.991	1.014	1.021	1.038							
Mn	0.007	0.007	0.009	0.010	0.009	0.007	0.013	0.010	0.014	0.010	0.009	0.011	0.007	0.011	0.015	0.009	0.009	0.012	0.010	0.010	0.012	0.011	0.010	0.014							
Mg	1.067	1.063	1.088	1.038	1.057	1.078	0.946	0.990	0.917	1.016	1.028	0.957	1.037	0.929	0.946	0.961	1.069	0.948	0.954	1.091	0.918	0.921	0.934	0.822							
Ca	0.013	0.010	0.010	0.011	0.012	0.011	0.015	0.012	0.009	0.014	0.011	0.014	0.010	0.012	0.011	0.011	0.015	0.017	0.009	0.012	0.012	0.012	0.025								
Na	0.000	0.001	0.000	0.000	0.000	0.001	0.000	0.001	0.000	0.000	0.000	0.000	0.000	0.000	0.000	0.000	0.002	0.001	0.000	0.001	0.000	0.000	0.019								
K	0.000	0.000	0.000	0.000	0.000	0.000	0.000	0.000	0.000	0.000	0.000	0.000	0.000	0.000	0.000	0.000	0.001	0.001	0.000	0.001	0.001	0.003	0.001								
Ni	0.000	0.001	0.002	0.000	0.000	0.000	0.001	0.000	0.000	0.000	0.001	0.000	0.000	0.000	0.000	0.000	0.000	0.000	0.000	0.000	0.000	0.000	0.000								
Σ	3.996	4.000	3.994	4.000	4.001	4.000	4.001	4.001	3.998	4.000	3.997	4.000	3.994	4.000	3.999	4.000	3.999	4.000	3.998	4.000	4.000	4.001	3.999								
Al ^{IV}	0.046	0.049	0.035	0.061	0.069	0.061	0.055	0.032	0.022	0.043	0.031	0.018	0.021	0.077	0.046	0.038	0.044	0.043	0.054	0.056	0.083	0.042	0.018	0.067							
Al ^{VI}	0.047	0.046	0.041	0.035	0.009	0.024	0.037	0.027	0.025	0.014	0.015	0.016	0.029	0.020	0.023	0.014	0.000	0.014	0.017	0.029	0.031	0.039	0.018	0.070							
Fs	44.50	45.03	43.72	46.51	46.25	44.78	51.02	49.19	52.97	48.08	47.53	51.01	46.64	52.40	51.52	51.03	46.11	51.44	50.98	43.99	52.33	52.35	52.15	55.40							
En	54.83	54.46	55.77	52.93	53.14	54.67	48.22	50.20	46.57	51.21	51.92	48.28	52.85	46.99	47.92	48.41	53.34	47.81	48.16	55.55	47.05	47.04	47.24	43.29							
Wo	0.67	0.51	0.51	0.56	0.60	0.56	0.76	0.61	0.46	0.71	0.56	0.71	0.51	0.61	0.56	0.55	0.55	0.76	0.86	0.46	0.62	0.61	0.61	1.32							
mg#	55.40	54.94	56.31	53.51	53.71	55.17	48.91	50.77	47.12	51.84	52.45	48.90	53.32	47.54	48.56	48.91	53.88	48.47	48.82	56.09	47.64	47.60	47.77	44.19							

En

60 50 40 30 20 10 0

Fs

- CNW: natural graywacke, 10kbar, XH₂O=0.25
- SkJ: 19.4Ann55.7+48.2An24.3+30Qtz+1.8Ed58, 10kbar
- PDB: 37.2Ann32+26.5An42+34.3Qtz, 12.5kbar
- PDB: 37.2Ann32+26.5An42+34.3Qtz, 15kbar
- SiJ: 20Ann50+50An45+30Qtz, 10kbar
- MV: 25Ann42.5+32An22+41Qtz, 5kbar
- MV: 25Ann42.5+32An22+41Qtz, 8kbar
- MV: 25Ann42.5+32An22+41Qtz, 10kbar
- This study

Fig. 4. Comparison of Opx 1 and orthopyroxene compositions which coexist with garnet+melt at moderate to high pressure conditions in experiments in Wo-En-Fs space. Some important characters of orthopyroxene formed by melting are revealed, viz., it ranges from En₄₀ to En₆₀ depending on composition of starting material; it changes responding to the temperature for the same starting material. CNW: Conrad et al. (1988); SkJ: Skjerlie and Johnston (1993); PDB: Patiño Douce and Beard (1995); SiJ: Singh and Johannes (1996b); MV: Montel and Vielzeuf (1997). SkJ and SiJ are operated on the system of tonalitic composition, while others are on metagraywacke.

Table. 3. Representative chemical analyses of plagioclase lamella in Opx 2. Formula unit normalized by O=8. \$: iron as total.

RockType	Leucosome/Pl lamella		
Sample	9610A		
Anal. No.	61	73	74
SiO ₂	53.91	55.15	54.50
TiO ₂	0.00	0.00	0.02
Al ₂ O ₃	29.49	29.06	29.08
Cr ₂ O ₃	0.00	0.00	0.00
\$FeO	0.72	0.57	0.73
MnO	0.00	0.00	0.09
MgO	0.03	0.00	0.02
CaO	11.95	10.77	10.77
Na ₂ O	4.71	5.40	5.30
K ₂ O	0.18	0.31	0.37
P ₂ O ₅	0.02	0.02	0.02
NiO	0.00	0.00	0.06
total	101.00	101.28	100.96
Si	2.421	2.462	2.447
Ti	0.000	0.000	0.001
Al	1.561	1.529	1.539
Cr	0.000	0.000	0.000
\$Fe	0.027	0.021	0.028
Mn	0.000	0.000	0.003
Mg	0.002	0.000	0.001
Ca	0.575	0.515	0.518
Na	0.410	0.467	0.462
K	0.010	0.018	0.021
P	0.001	0.001	0.001
Ni	0.000	0.000	0.002
Σ	5.007	5.013	5.023
Al ^{IV}	0.579	0.538	0.553
Al ^{VII}	0.982	0.991	0.986
An	57.77	51.50	51.7
Ab	41.20	46.70	46.12
Or	1.03	1.80	2.10

ilmenite and plagioclase lamellae. The ilmenite lamella, which cannot be analyzed because of its fineness, is confirmed by the compositional tie-line with host Opx 2 (Fig. 5). The plagioclase lamella is little higher in Ca (An₅₁₋₅₈) compared with the matrix plagioclase (Table. 3 and 7).

Garnet: Garnet, which generally occurs in the mesosome, is enriched in Fe (Alm₆₅Prp₂₅; FeO=28.01-30.81 wt%) and show slight zoning, with Ca increasing towards the rim (from 2.55 to 3.62 wt %). Garnet porphyroblast tends to be enriched in magnesium (Alm₆₄Prp₂₆; MgO=6.76 wt% in average; core portion), with Ca increasing towards the rim (from 2.44 to 3.53 wt%) (Fig. 6A; Table. 4). Some of the garnet porphyroblast maintain a zoning with respect to Mg and Fe, which slightly decrease towards the rim. The garnet porphyroblast in the mesosome of the veined migmatite is similar to that of Montel and Vielzeuf (1997) and Stevens et al. (1997) for Grs content, and to that of Conrad et al. (1988) in the Alm/Prp ratio (Fig. 7). The garnet from the "melanosome"-like zone between the mesosome and the leucosome

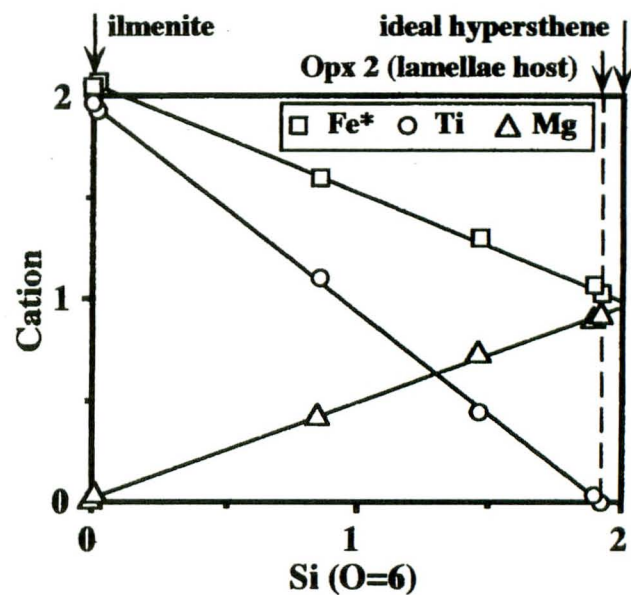


Fig. 5. Examination of exsolution lamella by the mixing test, where the results of point analyses are plotted, being normalized on the basis of O=6. Those with Si = 0.014, 0.850, 1.462 and 1.896 correspond to the analysis that include lamella and in host Opx 2 random ratios. The tie lines indicate the composition of ilmenite as an appropriate phase for lamella.

has also similar composition with them, but garnet in the diatexite is more iron rich (~Alm₆₆Prp₂₂; FeO < 31.16 wt%) (Fig. 6B; Table. 4).

The retrograde garnet rimming Opx 2 is ~Alm₆₉Prp₂₀ (Table. 5). Three representative chemical traverses (Fig. 8) characterize significant variations, especially in Fe and Al. Characteristic Fe-increase at around 0.1-0.15 mm from the contact with Opx 2 is recognized in zone 1. Fe and Mg strongly decrease, but Ca and Al increase in zone 2. They suggest the formation of the garnet by means of a net transfer reaction.

***Biotite:** The total tetrahedral Si+Al, less than 8, is assumed to indicate the presence of other element(s) in the tetrahedral site. The Opx 1, containing very limited amount of Fe³⁺, equivalent to 2% of total Fe, and the ilmenite+pyrite assemblage implying low oxygen fugacity, suggest a very limited amount of Fe³⁺ in the biotite. Deficiency in the tetrahedral site is thus considered to be fulfilled by Ti (see Farmer and Boettcher, 1981).

* As fluorine was not analyzed for some biotite in this study, all values discussed in the text and in Fig. 10 are calculated based on O=22 (not O, OH, F=24), expelling fluorine data. Although the cation number-based normalization can avoid the problem, it is not utilized because it results in overestimation of the octahedral site and the effect on evaluation of substitution (Dymek, 1983). The formulae listed in Table. 6 are calculated including fluorine based on O, OH, F=24.

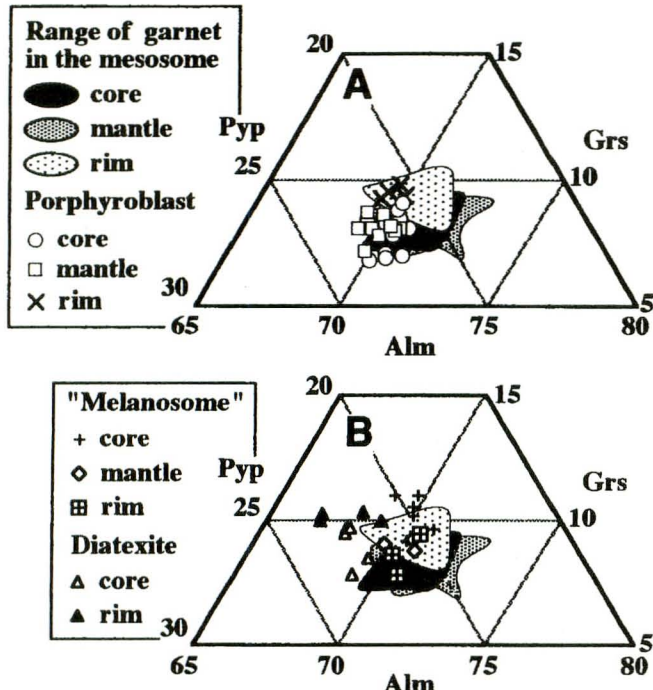


Fig. 6. Garnet compositions from the veined migmatite and the diatexite. A: comparison of the compositions of garnet generally occurring in the mesosome and porphyroblast. B: comparison of the composition of garnet generally occurring in the mesosome and in "melanosome"-like zone along the border between mesosome and leucosome, and in the diatexite.

Biotites which occur in the matrix isolated from other mafic minerals and included in coarse-grained feldspars have a common chemical composition, i.e., those in the mesosome are characterized by higher mg# ($Mg \times 100 / (Mg + Fe)$) of 60.25-69.04 with lower $^{[4]}Al$, and those in the leucosome have lower mg# of 53.56-60.60 and higher $^{[4]}Al$. The highest mg# (72.01-74.86) is detected from the biotite included in garnet porphyroblast. Symplectic biotite in the diatexite marks wide range of mg# (60.58-73.18). Responding to the order of mg#, the F contents (wt %) increase from 1.05-1.45 in the leucosome, 1.27-1.55 in the mesosome and 1.29-2.03 in garnet porphyroblast, as illustrated by Guidotti (1984) (Fig. 9, Table. 6).

Ti in the tetrahedral site seems emphasized in the biotite included in garnet porphyroblast than in other types of biotite. Ti shows negative 1:1 relation with Si representing a substitution,

$$^{[4]}Si = ^{[4]}Ti \quad (\text{Abrecht and Hewitt, 1988}) \quad (4)$$

The relation of tetravalent and tetrahedral element ($^{[4]}R^{2+} = ^{[4]}Ti + ^{[4]}Si$) and other elements of biotite in the mesosome (Fig. 10A, B) implies a substitution expressed as;

$$2.5^{[6]}R^{2+} + ^{[4]}Al = ^{[6]}Ti + 1.5^{[6]} \square + ^{[4]}R^{4+} \quad (5)$$

where $R^{2+} = Fe^{2+} + Mn + Mg$. This can be obtained by addition of substitutions,

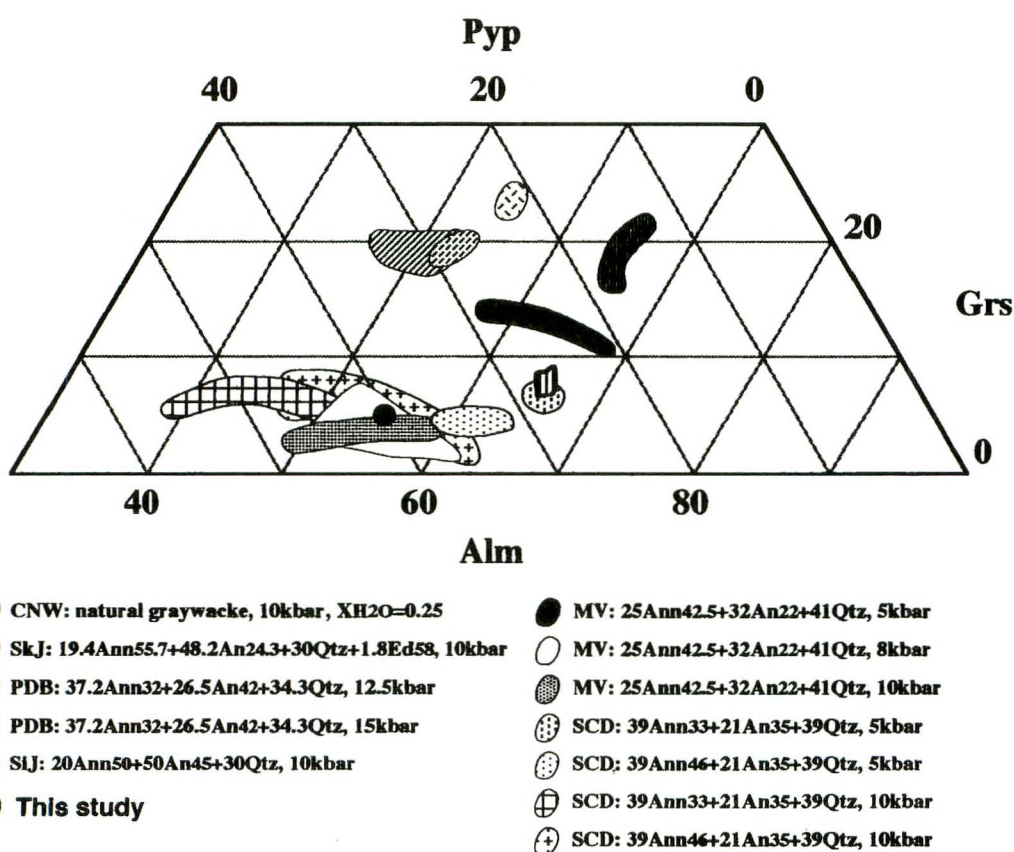


Fig. 7. Comparison of garnet porphyroblast and those from experiments in metaluminous system in Grs-Prp-Alm space. It is revealed that garnet composition basically depends on the chemistry of starting material, and Fe-Mg variation strongly depends on temperature. These characters are similar to those of orthopyroxene. Abbreviations of the references are as in Fig. 6 except SCD representing Stevens et al. (1997).

Table. 4. Representative chemical analyses of garnet. Formula unit normalized by O=12. Analytical positions are same as in Table. 1. Analytical numbers with "PB" are for porphyroblast.

RockType	Mesosome												"melanosome"								Diatexite				
	Sample 950804-1				950804-1-2				950825-1-2				950822-1d												
Anal. No.	i3	i5	i4	PB15	PB20	PB25	c2	c3	c1	aPB3	aPB2	aPB1	g7	g6	g1	g'3	g'2	g'1	a3	a2	a1	k3	k1	k4	
Anal. Pos.	c	m	r	c	m	r	c	m	r	c	m	r	c	m	r	c	m	r	c	m	r	c	m	r	
SiO ₂	38.98	38.72	38.87	39.28	38.91	39.06	38.86	38.77	38.83	38.39	38.42	38.52	35.82	38.43	38.53	38.67	38.64	38.68	38.64	38.89	39.01	39.92	38.68	38.76	
TiO ₂	0.06	0.05	0.06	0.00	0.05	0.07	0.05	0.03	0.02	0.05	0.06	0.01	0.04	0.04	0.01	0.04	0.05	0.05	0.06	0.03	0.05	0.02	0.05	0.05	
Al ₂ O ₃	21.98	22.01	21.89	22.26	22.23	22.09	21.86	22.00	21.78	21.86	21.88	22.05	21.80	21.82	21.55	21.81	21.87	21.98	22.01	21.70	21.82	22.17	21.93	22.00	
Cr ₂ O ₃	0.11	0.05	0.04	0.02	0.00	0.00	0.01	0.05	0.04	0.00	0.00	0.00	0.07	0.02	0.01	0.05	0.06	0.04	0.05	0.04	0.04	0.02	0.08	0.04	
FeO	29.72	29.72	29.36	29.37	29.09	30.38	29.68	30.00	29.12	29.73	29.16	27.95	29.44	28.61	30.18	29.36	29.48	29.51	31.16	29.96	30.34	30.08	30.60	31.03	
MnO	0.78	0.99	0.98	0.95	0.92	0.94	0.90	0.90	0.86	0.96	0.90	0.82	0.86	0.89	0.88	0.94	0.74	0.90	1.09	1.05	1.04	1.06	0.94	0.99	
MgO	6.56	6.57	6.39	6.85	6.68	6.26	6.56	6.45	6.26	6.85	6.87	6.60	6.70	6.54	6.26	6.68	6.39	6.30	5.86	5.41	5.86	5.86	5.67	5.69	
CaO	3.14	3.07	3.28	2.59	2.95	3.16	2.74	2.54	3.15	2.77	2.74	3.32	2.73	3.11	3.43	3.05	3.23	3.74	2.76	2.87	3.66	3.51	3.42	3.46	
Na ₂ O	0.00	0.00	0.00	0.00	0.00	0.01	0.00	0.00	0.04	0.00	0.00	0.00	0.00	0.00	0.00	0.00	0.01	0.02	0.01	0.00	0.03	0.01	0.00	0.00	
K ₂ O	0.00	0.00	0.00	0.00	0.00	0.00	0.00	0.00	0.00	0.00	0.00	0.00	0.00	0.00	0.00	0.00	0.00	0.00	0.00	0.00	0.00	0.00	0.00	0.00	
P ₂ O ₅	0.00	0.01	0.01	0.00	0.03	0.00	0.00	0.01	0.03	0.00	0.00	0.02	0.00	0.00	0.02	0.01	0.00	0.06	0.05	0.02	0.04	0.00	0.03	0.06	
NiO	0.02	0.03	0.00	0.01	0.00	0.00	0.00	0.05	0.02	0.00	0.01	0.04	0.00	0.07	0.00	0.01	0.00	0.00	0.00	0.00	0.01	0.00	0.00	0.00	
total	101.35	101.23	100.87	101.35	100.85	101.94	100.67	100.80	100.11	100.61	100.07	99.33	101.15	99.53	100.88	100.62	100.47	101.23	101.70	99.98	101.87	101.69	101.42	102.08	
Si	3.004	2.991	3.009	3.016	3.003	3.001	3.013	3.005	3.024	2.984	2.994	3.010	3.002	3.007	2.998	3.001	3.004	2.989	2.989	3.040	3.006	3.000	2.997	2.998	
Ti	0.004	0.003	0.004	0.000	0.003	0.004	0.003	0.002	0.001	0.003	0.003	0.001	0.002	0.002	0.001	0.002	0.003	0.001	0.003	0.000	0.003	0.001	0.003	0.003	
Al	1.996	2.005	1.997	2.014	2.022	2.001	1.998	2.003	1.999	2.003	2.010	2.031	2.002	2.012	1.977	1.995	2.004	2.003	2.006	2.000	1.982	2.014	2.003	1.999	
Cr	0.006	0.003	0.002	0.001	0.000	0.000	0.003	0.002	0.002	0.000	0.000	0.004	0.001	0.001	0.003	0.004	0.002	0.003	0.000	0.002	0.001	0.005	0.003		
Fe	1.916	1.920	1.900	1.886	1.878	1.952	1.925	1.945	1.896	1.932	1.901	1.826	1.919	1.872	1.964	1.906	1.916	1.908	2.016	1.960	1.955	1.939	1.983	2.001	
Mn	0.051	0.065	0.064	0.062	0.060	0.061	0.059	0.059	0.057	0.063	0.059	0.054	0.057	0.059	0.058	0.062	0.049	0.058	0.071	0.070	0.068	0.069	0.062	0.065	
Mg	0.754	0.757	0.737	0.784	0.769	0.717	0.758	0.745	0.726	0.793	0.798	0.769	0.778	0.763	0.726	0.772	0.740	0.726	0.676	0.630	0.674	0.673	0.655	0.654	
Ca	0.260	0.254	0.272	0.213	0.244	0.260	0.228	0.211	0.263	0.230	0.229	0.278	0.228	0.261	0.286	0.253	0.269	0.310	0.229	0.240	0.302	0.290	0.284	0.286	
Na	0.001	0.000	0.001	0.000	0.001	0.000	0.001	0.000	0.000	0.000	0.000	0.000	0.000	0.000	0.000	0.000	0.000	0.003	0.000	0.000	0.004	0.002	0.000		
K	0.00	0.00	0.00	0.00	0.00	0.00	0.00	0.00	0.00	0.00	0.00	0.00	0.00	0.00	0.00	0.00	0.00	0.00	0.00	0.00	0.00	0.00	0.00	0.00	
P	0.000	0.001	0.001	0.000	0.002	0.000	0.000	0.001	0.002	0.000	0.000	0.001	0.000	0.000	0.001	0.000	0.004	0.003	0.000	0.003	0.000	0.002	0.000	0.004	
Ni	0.001	0.002	0.000	0.001	0.000	0.000	0.003	0.001	0.000	0.000	0.003	0.000	0.004	0.000	0.001	0.000	0.000	0.000	0.000	0.001	0.000	0.000	0.000	0.000	
Σ	7.993	8.001	7.987	7.977	7.982	7.996	7.985	7.986	7.971	8.010	8.000	7.973	7.992	7.981	8.012	7.996	7.989	8.002	7.999	7.940	7.995	7.992	7.996	8.003	
Alm	64.27	64.09	63.91	64.04	63.64	65.28	64.81	65.71	64.45	64.02	63.64	62.38	64.35	63.35	64.73	63.68	64.43	63.56	67.38	67.59	65.19	65.26	66.45	66.57	
Sps	1.71	2.17	2.15	2.11	2.03	2.04	1.99	1.99	1.94	2.09	1.98	1.84	1.91	2.01	1.91	2.07	1.65	1.93	2.37	2.41	2.27	2.32	2.08	2.16	
Prp	25.29	25.27	24.79	26.62	26.06	23.98	25.52	25.27	25.17	24.68	26.28	26.72	26.27	26.09	25.82	23.93	25.79	24.88	24.18	22.59	21.72	22.65	21.95	21.76	
Grs	8.72	8.48	9.15	7.23	8.27	8.70	7.68	7.13	8.94	7.62	7.67	9.50	7.65	8.83	9.43	8.45	9.05	10.33	7.65	8.28	10.07	9.76	9.52	9.51	

Table. 5. Representative chemical analyses of retrograde garnet. Formula unit normalized by O=12. Traverses b-1 and 2 correspond to those in Fig. 8. Analytical positions are in respect of Opx 2 and plagioclase. Analytical zones are referred to in text.

Sample	10ATr. b-1												10ATr. b-2												950825-1-2			
	Anal. No.	119	126	121	122	124	125	118	128	135	136	129	130	131	132	133	127	b10	b4	Opx	Pl	→	Pl	→	Opx	→	Pl	
SiO ₂	37.79	37.59	37.63	37.60	38.17	38.42	38.02	37.10	38.12	37.71	37.70	37.58	38.11	37.56	38.00	37.95	38.28	38.42										
TiO ₂	0.08	0.00	0.01	0.02	0.00	0.01	0.01	0.00	0.02	0.00	0.03	0.04	0.03	0.02	0.00	0.02	0.00	0.00	0.00	0.00	0.00	0.00	0.00	0.00	0.00	0.00		
Al ₂ O ₃	21.93	22.24	22.00	22.26	22.31	22.26	22.27	21.90	22.44	22.44	22.39	22.24	22.31	22.26	22.43	22.25	21.72	21.61										
Cr ₂ O ₃	0.05	0.00	0.08	0.00	0.00	0.00	0.00	0.00	0.11	0.00	0.00	0.01	0.00	0.00	0.03	0.00	0.00	0.00	0.07	0.00								
FeO	32.20	33.24	32.65	32.75	32.91	32.07	31.22	31.36	32.48	33.44	32.26	32.46	32.45	32.29	31.45	32.27	31.18	29.61										
MnO	1.13	1.17	1.03	0.97	1.06	1.05	0.91	1.18	1.10	1.02	1.16	0.98	1.09	0.86	0.88	0.91	0.87	0.81										
MgO	4.63	4.89	5.07	5.04	5.02	4.99	4.53	4.31	4.95	4.94	5.02	5.07	4.87	4.														

Table. 6. Representative chemical analyses of biotite. Formula unit normalized by O, OH, F=24 except for biotite in the diatexite normalized by O=22. m: matrix; i: inclusion in garnet porphyroblast; s: symplectite for occurrence.

RockType	Mesosome								Leucosome						Diatexite					
Sample	9650								950825-1						950822-1d					
Anal. No.	3	5	6	8	9	n1	n1-2	n4	n1-3	d4	d4-5	e3	e2	h1	h4	b1	b1-5	b6	b6-5	b7
Occurrence	m	m	m	m	m	i	i	i	i	m	m	m	m	m	s	s	s	s	s	
SiO ₂	37.23	37.75	37.49	37.83	37.18	39.15	37.96	38.21	37.85	37.13	37.20	36.62	36.55	37.52	36.89	39.33	38.84	38.21	38.27	38.80
TiO ₂	4.99	5.17	5.63	5.38	5.12	6.72	6.61	6.68	7.12	5.64	5.47	6.02	5.77	5.48	5.79	4.11	4.31	4.87	4.86	4.99
Al ₂ O ₃	13.64	13.82	13.51	13.53	13.53	13.07	13.17	13.54	13.69	13.73	13.65	13.65	13.48	13.73	13.89	13.27	13.50	13.15	13.09	13.24
Cr ₂ O ₃	15.06	12.72	15.01	14.16	14.64	10.58	10.45	11.07	11.13	17.62	17.54	16.41	16.93	15.29	16.07	12.27	12.35	13.38	12.95	12.63
FeO	0.00	0.00	0.07	0.09	0.00	0.00	0.09	0.04	0.09	0.00	0.02	0.15	0.00	0.04	0.04	0.01	0.00	0.03	0.00	0.01
MnO	13.99	15.91	13.88	14.01	14.09	15.85	16.09	16.51	16.06	12.59	12.47	12.26	12.26	13.18	13.03	17.55	17.10	16.01	16.20	16.02
MgO	0.00	0.01	0.12	0.07	0.03	0.08	0.00	0.03	0.13	0.08	0.05	0.00	0.00	0.08	0.04	0.02	0.01	0.04	0.00	0.00
CaO	0.06	0.05	0.00	0.03	0.08	0.14	0.24	0.19	0.16	0.01	0.00	0.05	0.01	0.02	0.06	0.10	0.03	0.05	0.06	0.04
Na ₂ O	10.83	10.47	10.57	10.96	10.96	11.05	10.81	11.30	11.05	10.96	10.90	10.84	10.74	10.92	10.96	9.89	10.24	10.68	10.70	10.35
K ₂ O	0.00	0.00	0.00	0.00	0.00	0.00	0.00	0.00	0.00	0.00	0.00	0.00	0.00	0.00	0.00	0.00	0.03	0.00	0.02	0.00
NiO	0.01	0.10	0.01	0.00	0.07	0.08	0.00	0.00	0.05	0.09	0.03	0.11	0.06	0.07	0.13	0.00	0.00	0.05	0.04	0.07
ZnO	0.02	0.58	0.01	0.19	0.26	0.07	0.13	0.00	0.30	0.00	0.07	0.00	0.03	0.00	0.07	n.a.	n.a.	n.a.	n.a.	n.a.
P ₂ O ₅	0.09	0.00	0.06	0.04	0.00	0.00	0.03	0.00	0.00	0.00	0.02	0.00	0.00	0.00	0.06	0.00	0.00	0.00	0.01	0.00
F	1.31	1.55	1.43	1.32	1.42	2.03	1.67	1.77	1.29	1.22	1.05	1.12	1.38	1.45	1.13	n.a.	n.a.	n.a.	n.a.	n.a.
total	97.22	98.14	97.77	97.6	67.36	98.82	97.25	99.35	98.91	99.06	98.46	97.23	97.2	97.78	98.16	-	-	-	-	-
O=F	0.55	0.65	0.60	0.55	0.60	0.86	0.70	0.74	0.54	0.51	0.44	0.47	0.58	0.61	0.48	-	-	-	-	-
total	96.67	97.49	97.17	97.05	96.76	97.97	96.54	98.61	98.36	98.54	98.02	96.76	96.62	97.17	97.69	96.55	96.38	96.49	96.18	93.17
Si	5.506	5.470	5.503	5.554	5.496	5.571	5.499	5.440	5.422	5.460	5.499	5.465	5.464	5.523	5.441	5.724	5.681	5.639	5.654	5.702
Ti	0.555	0.564	0.622	0.594	0.569	0.719	0.720	0.715	0.767	0.623	0.608	0.676	0.648	0.606	0.642	0.450	0.475	0.540	0.540	0.552
Al	2.377	2.361	2.337	2.340	2.358	2.191	2.249	2.271	2.311	2.379	2.378	2.401	2.375	2.382	2.415	2.276	2.237	2.288	2.278	2.293
Cr	0.001	0.012	0.001	0.000	0.008	0.009	0.000	0.00	0.006	0.010	0.004	0.013	0.007	0.008	0.015	0.000	0.000	0.005	0.005	0.008
Fe	1.862	1.541	1.842	1.738	1.810	1.258	1.266	1.318	1.333	2.167	2.168	2.048	2.116	1.881	1.983	1.493	1.510	1.652	1.599	1.552
Mn	0.000	0.000	0.009	0.011	0.000	0.000	0.011	0.005	0.011	0.000	0.002	0.019	0.000	0.005	0.005	0.001	0.000	0.003	0.000	0.001
Mg	3.083	3.436	3.036	3.066	3.104	3.362	3.474	3.504	3.429	2.759	2.748	2.728	2.732	2.893	2.865	3.809	3.728	3.524	3.569	3.510
Ca	0.000	0.002	0.018	0.010	0.005	0.012	0.000	0.005	0.019	0.013	0.007	0.000	0.000	0.012	0.006	0.003	0.001	0.006	0.000	0.000
Na	0.016	0.015	0.000	0.009	0.022	0.039	0.066	0.053	0.044	0.002	0.000	0.013	0.001	0.006	0.017	0.028	0.008	0.015	0.016	0.012
K	2.042	1.936	1.980	2.053	2.067	2.005	1.998	2.052	2.019	2.055	2.055	2.064	2.049	2.050	2.062	1.836	1.911	2.011	2.017	1.941
Ni	0.000	0.000	0.000	0.000	0.000	0.000	0.000	0.000	0.000	0.000	0.000	0.000	0.000	0.000	0.000	0.000	0.000	0.003	0.000	0.003
Zn	0.002	0.062	0.001	0.020	0.028	0.007	0.014	0.000	0.031	0.000	0.008	0.000	0.003	0.000	0.007	0.000	0.000	0.000	0.000	0.000
P	0.012	0.000	0.007	0.004	0.000	0.000	0.004	0.000	0.000	0.000	0.003	0.000	0.000	0.000	0.007	-	-	-	-	-
F	0.612	0.712	0.662	0.611	0.661	0.914	0.766	0.796	0.585	0.565	0.490	0.528	0.650	0.676	0.528	-	-	-	-	-
Σ	15.455	15.399	15.355	15.401	15.466	15.175	15.300	15.364	15.392	15.469	15.480	15.427	15.396	15.366	15.467	15.620	15.641	15.686	15.680	15.574
mg#	62.35	69.04	62.24	63.82	63.17	72.77	73.29	72.67	72.01	56.01	55.90	57.12	56.35	60.60	59.10	71.84	71.17	68.08	69.06	69.34

Table. 7. Representative chemical analyses of plagioclase. Formula unit normalized by O=8. F: fine; M: medium; C: coarse; I: inclusion for grain size. Analytical positions are same as in Table. 1., except for g: in garnet; gp: in garnet porphyroblast. \$: iron as total.

RockType	Mesosome												Leucosome												Diateixte						
	Sample						950804-1			950804-1-2			950804-1-2			950825-1			950825-1-2			9610A-1			950822-1d						
Anal. No.	h1	m3	m4	f3	f2	127	f4	f6	i0	i0.5	i00	e9	e12	e10	g'8	g'7	g'6	51	180	179	e1	e1.5	e2	e18	e18.5						
GrainSize	I	F	F	M	M	I	C	C	F	F	F	C	C	C	M	M	M	I	I	I	C	C	C	M	M						
Anal. Pos.	g	c	r	c	r	gp	c	r	c	m	r	c	c	r	c	m	r	c	m	r	c	c	ge	M	M						
SiO ₂	53.00	57.21	57.05	55.92	56.08	56.10	55.69	55.62	56.29	55.33	55.94	57.38	57.13	56.18	56.06	56.67	56.11	55.12	54.70	54.94	56.64	55.95	56.30	56.43	58.38						
TiO ₂	0.00	0.04	0.01	0.02	0.02	0.01	0.00	0.00	0.00	0.01	0.00	0.01	0.02	0.04	0.00	0.03	0.01	0.04	0.00	0.00	0.02	0.04	0.01	0.00	0.00						
Al ₂ O ₃	30.64	27.45	27.95	27.85	27.95	28.94	27.15	27.38	27.79	27.87	28.02	28.20	28.37	27.58	27.52	27.57	28.79	28.33	28.01	27.74	27.80	27.96	27.80	27.64							
Cr ₂ O ₃	0.00	0.03	0.00	0.04	0.00	0.02	0.00	0.00	0.00	0.01	0.06	0.00	0.03	0.00	0.01	0.02	0.05	0.01	0.00	0.00	0.00	0.01	0.01	0.01	0.00	0.00					
\$FeO	0.24	0.05	0.03	0.00	0.04	0.00	0.18	0.06	0.03	0.02	0.05	0.01	0.06	0.08	0.00	0.04	0.00	0.06	0.00	0.05	0.03	0.18	0.21	0.01	0.00	0.00					
MnO	0.00	0.00	0.00	0.00	0.00	0.00	0.00	0.00	0.00	0.00	0.04	0.01	0.00	0.00	0.00	0.00	0.00	0.00	0.04	0.00	0.01	0.05	0.01	0.01	0.01	0.01					
MgO	0.02	0.00	0.01	0.00	0.01	0.01	0.02	0.00	0.00	0.01	0.00	0.00	0.01	0.00	0.00	0.01	0.00	0.01	0.00	0.00	0.00	0.00	0.00	0.00	0.00	0.00	0.00	0.02			
CaO	13.04	8.59	10.02	10.11	10.27	9.77	9.71	9.94	9.98	10.38	9.38	9.95	10.03	10.33	10.18	9.89	10.25	10.58	10.41	10.47	9.35	9.92	10.02	9.97	9.46						
Na ₂ O	3.95	5.66	5.80	5.67	5.59	5.69	5.83	5.75	5.83	5.59	5.73	5.98	5.82	5.62	5.05	5.67	5.68	5.20	5.56	5.18	6.04	5.88	6.01	5.92	5.95						
K ₂ O	0.10	0.31	0.24	0.24	0.20	0.26	0.29	0.23	0.21	0.25	0.18	0.23	0.18	0.14	0.21	0.24	0.18	0.28	0.26	0.22	0.21	0.20	0.24	0.27							
P ₂ O ₅	0.03	0.01	0.01	0.01	0.00	0.00	0.00	0.01	0.00	0.06	0.00	0.01	0.03	0.06	0.01	0.03	0.04	0.00	0.06	0.00	0.06	0.04	0.04	0.00	0.03						
NiO	0.01	0.00	0.03	0.00	0.00	0.00	0.00	0.00	0.00	0.00	0.00	0.00	0.00	0.04	0.04	0.00	0.00	0.00	0.10	0.04	0.00	0.03	0.00	0.07	0.00						
total	101.30	99.35	101.14	99.87	100.14	100.99	98.73	98.97	100.12	99.43	99.25	101.63	101.53	100.82	99.10	100.10	99.90	100.19	99.46	98.82	100.16	99.91	100.81	100.60	101.78						
Si	2.377	2.571	2.534	2.518	2.518	2.497	2.536	2.527	2.527	2.506	2.528	2.537	2.528	2.505	2.536	2.541	2.525	2.479	2.480	2.500	2.538	2.519	2.516	2.525	2.569						
Ti	0.000	0.001	0.000	0.001	0.001	0.000	0.000	0.000	0.000	0.000	0.000	0.000	0.001	0.001	0.001	0.000	0.000	0.000	0.000	0.000	0.001	0.001	0.000	0.000	0.000						
Al	1.620	1.454	1.463	1.478	1.479	1.519	1.457	1.466	1.470	1.484	1.484	1.460	1.471	1.491	1.470	1.454	1.463	1.526	1.514	1.503	1.465	1.475	1.473	1.466	1.433						
Cr	0.000	0.001	0.000	0.001	0.000	0.001	0.000	0.000	0.000	0.000	0.002	0.000	0.001	0.000	0.001	0.002	0.000	0.000	0.000	0.000	0.000	0.000	0.000	0.000	0.000						
\$Fe	0.009	0.002	0.001	0.000	0.001	0.007	0.002	0.001	0.001	0.001	0.002	0.000	0.002	0.003	0.000	0.002	0.000	0.002	0.000	0.002	0.000	0.002	0.001	0.007	0.008						
Mn	0.000	0.000	0.000	0.000	0.000	0.000	0.000	0.000	0.000	0.000	0.001	0.000	0.000	0.000	0.000	0.000	0.000	0.000	0.000	0.000	0.001	0.002	0.001	0.000	0.000						
Mg	0.001	0.000	0.000	0.000	0.001	0.000	0.000	0.001	0.000	0.000	0.000	0.000	0.000	0.000	0.001	0.000	0.000	0.001	0.000	0.000	0.000	0.000	0.000	0.000	0.000	0.000					
Ca	0.627	0.414	0.477	0.488	0.494	0.466	0.474	0.484	0.480	0.504	0.454	0.471	0.475	0.494	0.493	0.475	0.494	0.510	0.506	0.510	0.449	0.478	0.480	0.478	0.446						
Na	0.343	0.493	0.499	0.495	0.487	0.491	0.515	0.507	0.508	0.491	0.502	0.513	0.499	0.486	0.433	0.493	0.496	0.453	0.489	0.457	0.525	0.513	0.521	0.514	0.507						
K	0.006	0.018	0.014	0.014	0.011	0.015	0.017	0.013	0.012	0.014	0.011	0.013	0.010	0.008	0.012	0.014	0.010	0.016	0.015	0.013	0.012	0.012	0.014	0.015							
P	0.001	0.000	0.000	0.000	0.000	0.000	0.000	0.000	0.000	0.002	0.000	0.000	0.001	0.002	0.000	0.001	0.002	0.000	0.002	0.000	0.002	0.000	0.001	0.000	0.001						
Ni	0.000	0.000	0.001	0.000	0.000	0.000	0.000	0.000	0.000	0.000	0.000	0.002	0.001	0.000	0.000	0.000	0.000	0.037	0.002	0.000	0.001	0.000	0.002	0.000							
total	4.984	4.954	4.989	4.995	4.992	4.996	5.001	4.999	4.998	5.002	4.984	4.996	4.989	4.990	4.956	4.982	4.992	5.025	5.012	4.983	4.997	5.002	5.013	5.006	4.973						
Al ^{IV}	0.623	0.429	0.466	0.482	0.482	0.503	0.464	0.473	0.473	0.494	0.472	0.463	0.472	0.495	0.464	0.459	0.475	0.521	0.520	0.500	0.462	0.481	0.484	0.475	0.431						
Al ^{VII}	0.997	1.026	0.997	0.996	0.997	1.016	0.993	0.997	0.997	0.99	1.012	0.997	0.999	0.996	1.006	0.996	0.988	1.005	0.994	1.003	1.002	0.994	0.988	0.991	1.002						
An	64.24	44.76	48.18	48.95	49.80	47.94	47.12	48.21	48.00	49.95	46.95	47.24	48.27	50.00	52.00	48.37	49.40	52.08	50.07	52.08	45.49	47.66	47.38	47.51	46.07						
Ab	35.14	53.30	50.40	49.65	49.09	50.51	51.19	50.50	50.80	48.66	51.91	51.45	50.71	49.19	46.73	50.20	49.60	46.29	48.43	46.60	53.19	51.15	51.43	51.09	52.38						
Or	0.61	1.95	1.41	1.40	1.11	1.54	1.69	1.29	1.20	1.39	1.14	1.30	1.02	0.81	1.27	1.43	1.00	1.63	1.50	1.32	1.32	1.20	1.18	1.39	1.55						

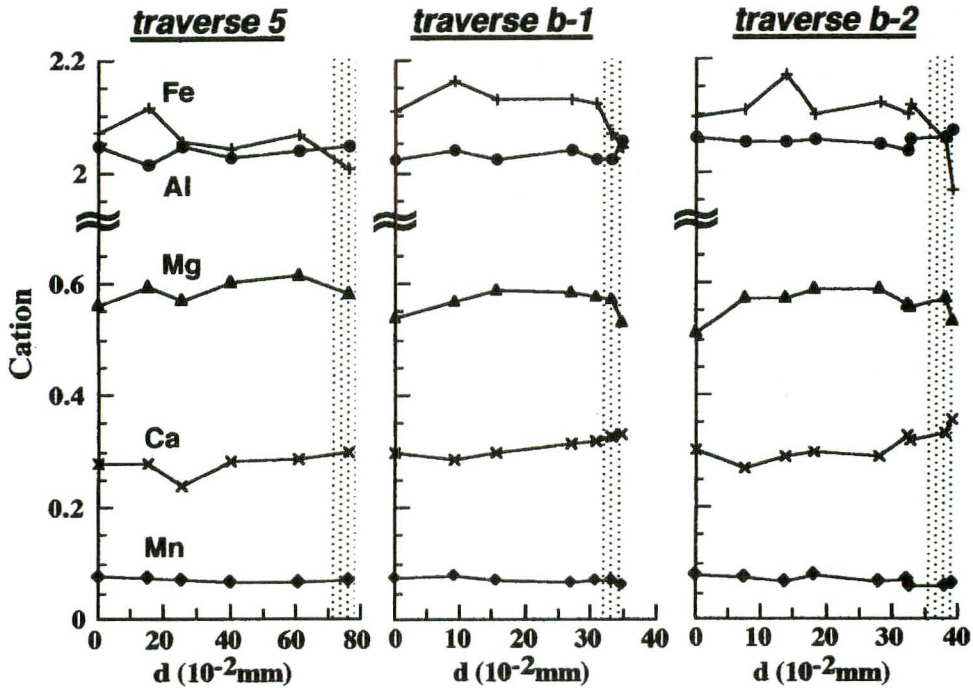


Fig. 8. Representative traverses of retrograde garnet corona. Lateral axis corresponds to the distance from the contact with Opx 2. Shaded area corresponds to zone 2 (see text). Traverse 5 is indicated in Fig. 2I.

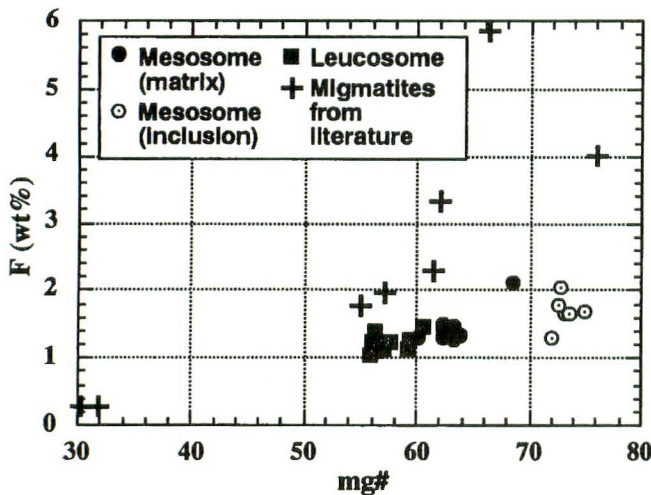


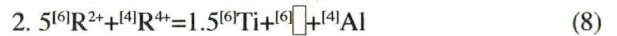
Fig. 9. A diagram of mg# against F contents of the biotite with those from literature for comparison. Note mg# and F portionally increase, and biotite inclusions in garnet porphyroblast of the present study contain less F compared to the literature's one with similar mg#. Data from Fitzsimons (1996), Braun et al. (1996), Dasgupta et al. (1992) and Mazurek (1992). All are from granulite terrains recording \sim 850-1000°C, except Mazurek (1992) with lowest mg# and F indicating \sim 650°C.



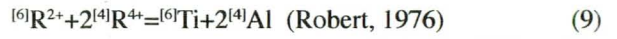
and,



For the biotite in the leucosome, on the other hand, the 2:1 negative relation of $^{[6]}R^{2+}$ and $^{[6]}Ti$ (Fig. 10C), and no variation in the tetrahedral site (Fig. 10D) indicates that it is simply controlled by substitution (6). The symplectitic biotite in the diatexite is characterized by a substitution,



which is a combined equation of



and eq. (6), judging from the trends in Fig. 10C and D.

Plagioclase: Plagioclases in the mesosome, leucosome and the diatexite are almost uniform in composition without zonation, and identified as andesine/labradorite ($An_{45-55}Ab_{43-53}$) (Table. 7). The composition is also similar for plagioclase occurring as inclusions in mafic minerals.

Accessory phases: Ilmenite generally contains a limited amount of Fe_2O_3 (< 0.05 p.f.u.) (Table. 8). Apatite included in garnet porphyroblast of the mesosome is slightly enriched in Fe compared to that in the leucosome matrix. The former contains 3.05-4.56 wt% F (Table. 9).

Bulk chemistry of the leucosome and the diatexite

The SiO_2 of the leucosome and the diatexite ranges from 64.24 to 68.24 wt%, and from 66.74 to 70.11 wt%, respectively. The leucosome has higher Ti, Al, Fe, Mn, Mg, V, Y,

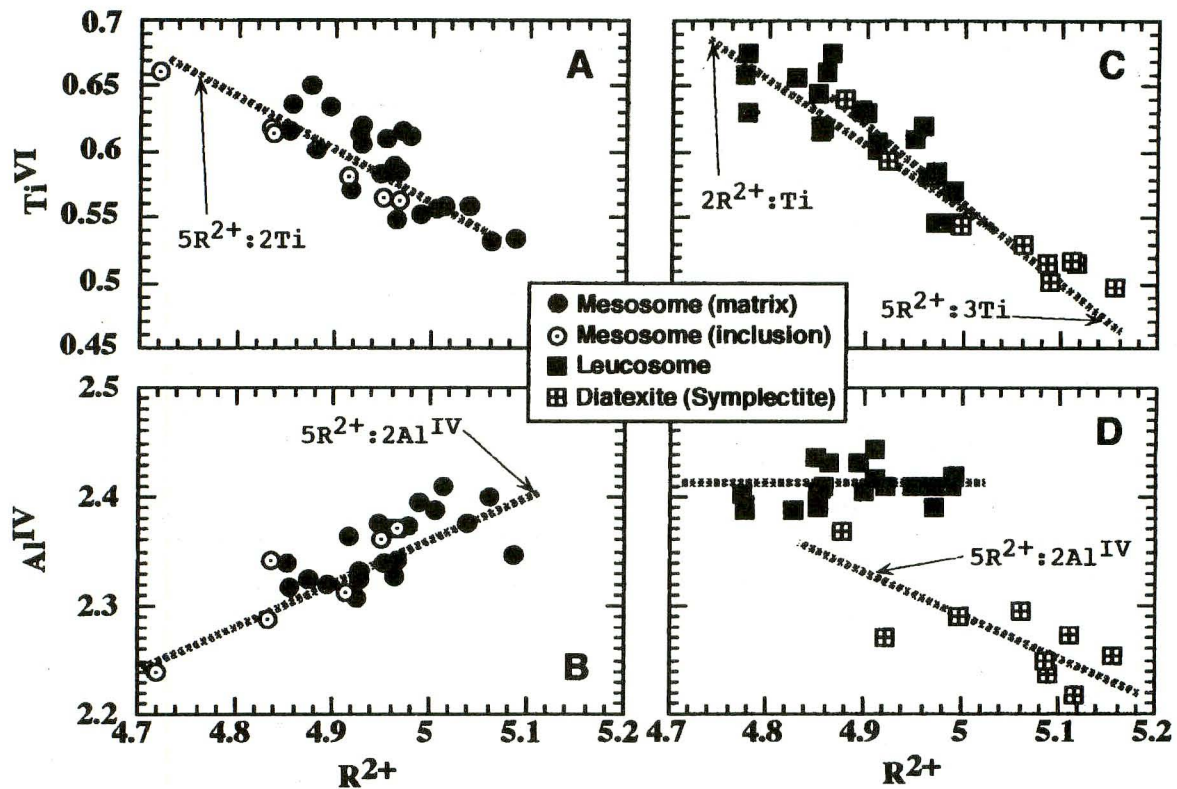


Fig. 10. A-D. Diagrams demonstrating the mode of chemical substitutions observed in the biotites in the veined migmatite and the diatexite. See text for details.

Table. 8. Representative chemical analyses of ilmenite. Formula unit normalized by O=3. m: matrix; r: retrograde for occurrence type. *: calculated.

RockType	Mesosome	Leucosome	Diatexite
sample	950804-1	950825-1-2	950822-1d
Anal. No.	c5	a20	d27
Occurrence	m	m	r
SiO ₂	0.03	0.01	0.02
TiO ₂	51.83	53.30	52.72
Al ₂ O ₃	0.02	0.00	0.01
Cr ₂ O ₃	0.10	0.07	0.10
*Fe ₂ O ₃	0.94	0.00	0.00
FeO	44.15	44.96	46.18
MnO	0.21	0.33	0.27
MgO	1.29	1.13	0.32
CaO	0.01	0.01	0.00
Na ₂ O	0.00	0.03	0.00
K ₂ O	0.00	0.00	0.00
NiO	0.00	0.00	0.00
total	98.58	99.84	99.62
Si	0.001	0.000	0.000
Ti	0.989	1.003	1.001
Al	0.001	0.000	0.000
Cr	0.002	0.001	0.002
Fe ³⁺	0.018	0.000	0.000
Fe ²⁺	0.936	0.941	0.975
Mn	0.005	0.007	0.006
Mg	0.049	0.042	0.012
Ca	0.000	0.000	0.000
Na	0.000	0.001	0.000
K	0.000	0.000	0.000
Ni	0.000	0.000	0.000
Σ	2.001	1.995	1.996

Table. 9. Representative chemical analyses of apatite. Formula unit normalized by O, F, OH=26 for those including fluorine analysis, and O=25 for others.

RockType	Mesosome			Leucosome			
	Sample	9616		Jem1	950825-1		
Anal. NO.		1	2	3	e3	e4	i1
SiO ₂	0.32	0.31	0.21	0.22	0.20	0.14	
TiO ₂	0.02	0.03	0.00	0.00	0.01	0.00	
Al ₂ O ₃	0.01	0.01	0.01	0.00	0.00	0.00	
Cr ₂ O ₃	0.00	0.00	0.02	0.01	0.00	0.03	
FeO	0.92	1.04	1.04	0.18	0.17	0.06	
MnO	0.14	0.07	0.01	0.00	0.03	0.03	
MgO	0.04	0.04	0.05	0.03	0.01	0.03	
CaO	54.85	55.23	55.59	55.68	56.16	56.41	
Na ₂ O	0.11	0.14	0.05	0.00	0.00	0.00	
K ₂ O	0.00	0.00	0.00	0.00	0.01	0.00	
NiO	0.00	0.01	0.00	0.01	0.04	0.04	
P ₂ O ₅	39.97	38.79	40.35	41.53	41.74	41.67	
ZnO	0.00	0.06	0.00	n.a.	n.a.	n.a.	
F	4.56	4.28	3.05	n.a.	n.a.	n.a.	
total	100.94	99.99	100.40	97.66	98.37	98.41	
O=F	1.92	1.80	1.28	-	-	-	
total	99.02	98.19	99.11	97.66	98.37	98.41	
Si	0.061	0.062	0.062	0.061	0.060	0.060	
Ti	0.003	0.004	0.000	0.000	0.001	0.000	
Al	0.002	0.002	0.003	0.000	0.000	0.000	
Cr	0.000	0.000	0.003	0.001	0.000	0.004	
Fe	0.132	0.151	0.149	0.025	0.024	0.008	
Mn	0.021	0.010	0.002	0.000	0.004	0.004	
Mg	0.010	0.009	0.014	0.008	0.002	0.007	
Ca	10.025	10.259	10.217	10.044	10.064	10.104	
Na	0.036	0.045	0.017	0.000	0.000	0.000	
K	0.000	0.000	0.001	0.000	0.002	0.000	
Ni	0.000	0.001	0.000	0.001	0.005	0.005	
P	5.773	5.693	5.860	5.920	5.910	5.898	
Zn	0.000	0.000	0.001	-	-	-	
F	2.457	2.346	1.655	-	-	-	
Σ	18.520	18.589	17.984	16.060	16.072	16.090	

Table. 10. Chemical composition of the leucosome and the diatexite of the GOBM in the Tekkali area. Fe₂O₃ as total iron. L.O.I.: Loss on Ignition; n.d.: not detected; Tzr: temperatures (°C) calculated for Zr-saturation of each samples utilizing Watson and Harrison (1983).

Rock Type	Leucosome								Diatexite		
	950803-1aL	950803-1bL	950803-2bL	950804-1L	950809-1aL	950819-6bL	950825-3bL	950902-1L	950730-1b	950822-1d	950827-2b
SiO ₂	68.24	64.24	65.07	65.69	66.89	67.36	66.07	67.21	70.11	67.93	66.74
TiO ₂	0.62	0.80	0.93	0.75	0.62	0.75	0.65	0.68	0.55	0.68	1.08
Al ₂ O ₃	14.68	14.73	14.88	14.67	14.89	14.41	14.68	14.73	14.32	14.41	14.43
Fe ₂ O ₃	5.56	7.22	8.17	7.01	5.55	7.01	6.56	6.06	4.71	5.08	6.24
MnO	0.10	0.12	0.15	0.11	0.09	0.13	0.11	0.12	0.08	0.07	0.07
MgO	1.67	2.25	2.33	2.08	1.78	1.90	1.98	1.75	1.61	1.81	1.70
CaO	3.84	3.77	4.39	3.56	3.75	3.60	3.61	3.82	3.31	3.26	3.97
Na ₂ O	2.03	1.91	1.99	1.91	2.36	1.94	2.14	1.87	1.80	2.03	2.41
K ₂ O	3.15	3.06	1.78	3.08	2.83	2.54	3.17	2.63	3.79	3.91	2.82
P ₂ O ₅	0.11	0.13	0.14	0.12	0.10	0.11	0.10	0.12	0.13	0.15	0.16
L.O.I.	0.40	0.31	0.22	0.51	0.26	0.31	0.23	0.30	0.17	0.29	0.15
total	99.98	98.22	99.83	98.98	98.87	99.74	99.06	98.99	100.40	99.33	99.62
Ba	557	556	421	526	510	494	559	511	942	706	749
Cr	50	44	76	57	46	63	39	40	47	40	40
Nb	8	11	12	11	10	14	9	9	9	9	18
Ni	13	14	29	16	10	35	13	16	17	14	31
Rb	106	95	57	99	115	85	109	104	115	131	101
Sr	207	185	166	181	207	159	179	181	159	155	189
V	95	131	143	126	99	120	111	90	86	89	121
Y	31	33	35	31	32	37	33	37	27	29	24
Zn	66	123	112	101	87	88	94	45	64	92	145
Zr	149	185	174	175	154	170	143	154	166	190	251
Cu	13	17	16	10	13	18	16	13	5	n.d.	13
A/CNK	1.07	1.11	1.13	1.13	1.08	1.15	1.09	1.15	1.10	1.07	1.01
A/NK	2.18	2.28	2.86	2.27	2.14	2.43	2.11	2.49	2.03	1.90	2.06
Fe/Mg+FeI	0.77	0.76	0.78	0.77	0.76	0.79	0.77	0.78	0.74	0.74	0.79
Tzr	824	842	839	824	827	840	819	827	837	846	869

and lower K, P, Ba, Rb contents in comparison with the diatexite. Other elements indicate mostly similar values for both. Although the almina-saturation index values of the leucosome and the diatexite are clustered around 1.1 (Table. 10), normative corundum is higher in the leucosome than in the diatexite (Table. 11). In comparison with granitic rocks with similar SiO₂ values (Whalen et al., 1987), it follows that the leucosome and the diatexite contain higher Ti, Fe, Mn, Mg, Ca than I-, S- and A-type granites. Al₂O₃ content and the resulting norm corundum are nearly similar to the S-type granite. Ti, Mn and Fe enrichment resembles that of Charnockite Magma Type (CMT; Kilpatrick and Ellis, 1992), giving rise to normative rutile and hematite (Table. 11). Some trace elements, for example, Ba (< ~700-940 ppm), Sr (< ~207 ppm) and V (< ~131-143 ppm) are particularly higher than granitic magma types. The trace element concentrations give a similar pattern to that of CMT in the primordial mantle-normalized spidergram (Fig. 11).

Temperature-pressure estimates

As the melting experiments have shown (cf. Fig. 4 and 7

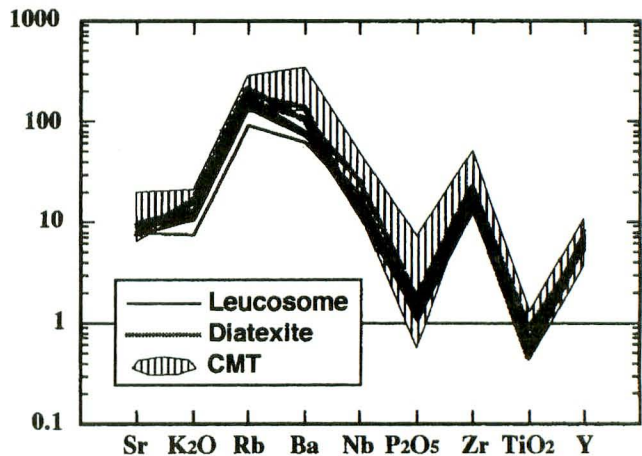


Fig. 11. Spidergrams of the leucosome and the diatexite normalized by the values of primordial mantle (referred from the values of data set No. 4, and No. 2 for P, of Table. 4.7 of Rollinson, 1993). The striped area indicating the CMT with the same level of SiO₂ contents with the leucosome and the diatexite. CMT data are from Kilpatrick and Ellis (1992) and Zhao et al. (1997).

Table. 11. Calculated norm composition of the leucosome and the diatexite, and of I-, S-, A-type granites and average CMT Ardery Charnockitic Intrusions. Abbreviations after Kretz (1983) except Di and Hyp for diopside and hypersthene, respectively. WCC (87); Whalen et al. (1987); K&E (92); Kilpatrick and Ellis (1992); -: not calculated.

Rock type	Leucosome							
	950803-1aL	950803-1bL	950803-2bL	950801-1L	950809-1aL	950819-6bL	950825-3bL	950902-1L
Qtz	33.97	30.35	34.20	32.40	31.92	36.12	31.08	35.81
Crn	1.21	1.73	2.03	2.01	1.37	2.19	1.40	2.15
Or	18.62	18.08	10.52	18.20	16.72	15.01	18.73	15.54
Ab	17.18	16.16	16.84	16.16	19.97	16.42	18.11	15.82
An	18.33	17.85	20.86	16.88	17.95	17.14	17.26	18.17
Di	-	-	-	-	-	-	-	-
Hyp	4.16	5.60	5.80	5.18	4.43	4.73	4.93	4.36
Mag	-	-	-	-	-	-	-	-
Ilm	0.21	0.26	0.32	0.23	0.19	0.28	0.23	0.26
Hem	5.56	7.22	8.17	7.01	5.55	7.01	6.56	6.06
Ttn	-	-	-	-	-	-	-	-
Rt	0.51	0.66	0.76	0.63	0.52	0.60	0.53	0.54
Ap	0.25	0.30	0.32	0.28	0.23	0.25	0.23	0.28
Rock type	Diatexite			I-type	S-type	A-type	CMT	
	950730-1b	950822-1d	950827-2b	-	-	-	-	
Qtz	36.01	31.90	31.34	28.06	33.17	30.19	26.80	
Crn	1.55	1.27	0.58	-	2.52	-	-	
Or	22.40	23.11	16.67	20.09	23.40	27.48	25.71	
Ab	15.23	17.18	20.39	26.49	20.39	34.44	22.00	
An	15.57	15.19	18.65	15.01	9.09	1.83	12.43	
Di	-	-	-	0.12	-	1.40	-	
Hyp	4.01	4.51	4.23	6.24	7.66	1.34	3.29	
Mag	-	-	-	1.51	0.81	1.80	-	
Ilm	0.17	0.15	0.15	0.82	0.91	0.49	0.23	
Hem	4.71	5.08	6.24	-	-	-	6.89	
Ttn	-	-	-	-	-	-	2.07	
Rt	0.46	0.60	1.00	-	-	-	0.29	
Ap	0.30	0.35	0.37	0.25	0.35	0.09	0.97	

and references cited therein), the relation between temperature/pressure conditions and chemical compositions of the hypersolidus phases generally follows that documented by thermodynamic and experimental calibrations for thermobarometric usage (e.g., Harley, 1984; Lal, 1993; Green, 1977; Newton and Perkins, 1983), although some experimental results disagree with it (cf., Patiño Douce and Beard, 1995). The Grt-Opx thermometer and the Grt-Opx-Pl-Qtz (GOPQ) barometer are, therefore, considered to be suitable for a melt-bearing system. The Grt-Opx thermometer by several authors were evaluated by interpolating the mineral data of melting experiments (Fig. 12). Thermometer by Lal (1993) appears to be the most appropriate. The merit of utilizing Lal (1993) is, furthermore, the availability of the internally consistent GOPQ barometer, and that its reliability can also be simultaneously checked (see Lal, 1993). Utilizing whole rock analysis, the Zr-saturation thermometer (Watson and Harrison, 1983) was also applied for the leucosome and the diatexite. Estimation of temperature-pressure conditions of the veined migmatite and the diatexite are attempted on:

- (1) a combination of core-compositions of garnet porphyroblast, Opx 1 and medium- to coarse-grained plagioclase in the mesosome for pressure and temperature conditions of the beginning of partial melting;
- (2) a combination of compositions of garnet rim, bulk

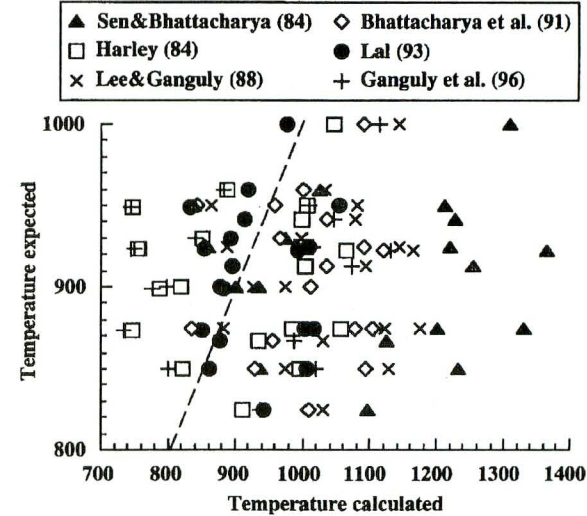


Fig. 12. Particular temperature conditions ("Temperature expected") at which the minerals equilibrated with melt in experimental studies are compared with temperature calculated by garnet-orthopyroxene thermometer interpolating their compositions (Temperatures in °C). Harley (1984) tends to indicate lower temperature, while Sen and Bhattacharya (1984) always estimate over 100–300°C (cf. Fitzsimons and Harley, 1995). Lee and Ganguly (1988) and Bhattacharya et al. (1991) show similar results, i.e., some are within < 100°C error range, but others are highly overestimated. 50% of the results of Lal (1993) shows good agreement with < 50°C error range. Ganguly et al. (1997), recently established calibration, results in values similar to those of Harley (1984). These observations indicate that Lal (1993) best estimates among all tested here. The data sets utilized are from Conrad et al. (1988), Sjølie and Johnston (1993), Patiño Douce and Beard (1995), Singh and Johannes (1996b) and Montel and Vielzeuf (1997).

Opx 2 and plagioclase rim in the diatexite to obtain the condition of the last reequilibrium before exsolution of Opx 2. The Zr-thermometer is expected to indicate the maximum for this condition because zircon is the near-liquidus phase, according to petrography; and

(3) a combination of adjacent compositions of zone 2 of retrograde garnet and Opx 2, and adjacent rim composition of plagioclase for minimum IBC pressure and temperature conditions for both the veined migmatite and diatexite.

As a result, condition (1) ranges from 5.6 to 6.8 kbar and 742 to 779°C. The estimated condition (2), ranging from 6.9 to 7.9 kbar and 837 to 906°C, by GOPQ thermobarometer is concordant with that by Zr-thermometer, ranging from 815 to 869°C, with temperature higher than ~840°C being obtained from the diatexite. The following isobaric cooling event records 5.2-6.0 kbar at 639-700°C and 6.0-6.3 kbar at 675-710°C, for condition (3) of the veined migmatite and the diatexite, respectively. Average values from GOPQ calculation for all the conditions are listed in Table. 12, and results from Zr thermometer are given in Table. 10.

Discussion of the nature of the thermal event in the Tekkali area

Implications from mineral chemistry: A migmatitic rock is a complex of phases equilibrated with melt, crystallized from melt, and even devoid of melting (*restite sensu stricto*) (cf. Osanai et al., 1997). This implies that a portion that seems to be neosome, possibly includes a part of palaeosome, and vice versa. The mesosome of the veined migmatite is also not an exception, as observed in the petrography. Because the mesosome is a portion with tiny veins of melt channels (Yamamoto et al., 1998), it should consist of minerals that originated in both subsolidus and hypersolidus conditions. Taking the example of plagioclase, that crystallized from the melt coexists with and/or forms a rim on that originally present in the protolith. The composition of the hypersolidus plagioclase is changed, depending on whether or not garnet coexists with it (Johannes, 1989; Patiño Douce and Beard, 1995; Stevens et al., 1997). The coarser-grained plagioclase in the mesosome of the GOBM is considered to be a product of *in-situ* growth from melt (Yamamoto et al., 1998), which is supported by the common composition of biotite in the matrix and in the plagioclase. Antiperthitic lamella, which tends to appear in coarser plagioclase, may be attributed to the originally less anorthitic nature of the plagioclase stabilized with garnet porphyroblast. The P-T condition estimated using garnet porphyroblast and Opx 1 is ~6.3 kbar and ~760°C. The pressure is consistent with Vielzeuf and Montel (1994) and Stevens et al. (1997), who recognized garnet with melt in 8 and 5 kbar runs, contrary to others showing garnet stability

at higher pressure conditions, e.g., ~>10 kbar (e.g., Sjkerlie and Johnston, 1993; Patiño Douce and Beard, 1995; Singh and Johannes, 1996a; b). Comparing pressure conditions and the resulting mineral compositions of experiments by Montel and Vielzeuf (1996) and Stevens et al. (1997) with those of the mesosome indicates that the possible protolith of the mesosome is metagraywacke.

Experimental as well as field evidences have shown that even in the metaluminous system with low aH₂O, melting starts at temperatures as low as ~700-780°C by dehydration breakdown of biotite (Le Breton and Thomson, 1988; Singh and Johannes, 1996a; Owen and Greenough, 1997). The melting fraction at this temperature range is limited to <~30% (Clemens and Vielzeuf, 1987; Holtz and Johannes, 1991; Wickam, 1987; Allibone and Norris, 1992). The temperature of 760°C, estimated for the melting of veined migmatite, permits a limited fertility of melt, which now forms leucocratic portions within the mesosome.

Although mg# of the biotite inclusions in garnet porphyroblast may be one of the indicators of high temperature (Guidotti, 1984; Stevens et al., 1997 and references therein), the effect of retrograde Fe-Mg exchange between biotite and garnet cannot be ignored. However, the higher Ti content of the biotite inclusions in garnet porphyroblast than in the matrix biotite in the mesosome is consistent with observations in the literature, which emphasize their proportional trend to temperature (Singh and Johannes, 1996b; Stevens et al., 1997 and references therein). Al in the mesosome biotite changing against Ti is also a feature often reported, although it is usually for octahedral Al (e.g., Montel and Vielzeuf, 1997; Stevens et al., 1997). The highest F in the biotite inclusions in the present study indicates that the biotite breakdown contributed to the melting, but it is still lower than in biotite of the migmatite formed at ~850-1000°C (Fig. 9). This implies that either the biotite is less dehydrated during melting or that it experienced less heat events to release OH. The latter case is not favored by the less F content in the matrix biotite of the mesosome. The former case is then feasible, with the assumption of relatively low temperature together with the presence of external H₂O, which set a temperature condition below biotite-out and fertility of melt restricted. The plutonic diatexite is a probable reservoir of heat and H₂O necessary to induce incipient melting in the mesosome, originally metagraywacke.

Heat source and thermal event in the Tekkali area: Yamamoto et al. (1998) deduced a migmatization process in the Tekkali area as follows: the melt that was initiated and percolated into the mesosome of the veined migmatite was partly segregated and created the leucosome, leaving a part of it within the mesosome, and the plutonic diatexite resulted from advanced melting. This interpretation, however, seems to

Table. 12. Average of temperature-pressure estimation resulted from GOPQ assemblage of the veined migmatite and the diatexite, and dT/dP calculated from P-T values for both lithologies.

	Veined migmatite		Diatexite	
	Peak(n=10)	Retro(n=4)	Peak(n=8)	Retro(n=6)
P (kbar)	6.2	5.5	7.5	6.2
T (°C)	756	657	877	689
dT/dP	128		138	

involve a pitfall, namely that the garnet porphyroblast and Opx 1, which are the representative phases formed during partial melting, do not appear in the plutonic diatexite. If these minerals formed in the mesosome when underplated magma crystallized providing heat and H_2O to the metagraywacke (parental rock of the mesosome), they are not necessarily contained in the magma, i.e., diatexite. The garnet in the diatexite is considered to have trapped from the mesosome when the diatexite magma was emplaced. Some of them have altered in chemical composition from those in the mesosome due to reequilibrium, and others have resulted in the formation of the symplectic biotite, which contains higher Fe and lower Al than other biotites indicating exchange of these elements with melt (Abdel-Rahman, 1994). The Zr-saturation temperature of the leucosome, which is similar but slightly lower than that of the diatexite, suggests that the leucosome has been generated from the same magma as the diatexite and that it plays a role in inputting heat into the metagraywacke. The chemistry of the leucosome and the diatexite is similar to that of CMT. High Ti in biotite indicates its high temperature of formation, and the presence of lamellae in the Opx 2 implies a specific temperature history of the magma, as inverted pigeonite in typical CMT (Kilpatrick and Ellis, 1992). Even a “dry” granulite, which had been considered with very limited aH_2O , possibly contains a higher amount of water, if without other vapor species (for example, brines) (Aranovich and Newton, 1998). Micro FTIR analysis of dusty inclusions in garnet porphyroblast detected aqueous species, but neither CO_2 nor CH_4 (Niimi and Yamamoto, 1998). The high temperature ($\sim 880^\circ C$) CMT intruded and created the diatexite at the pressure of ~ 7.5 kbar indicating a crustal level deeper than ~ 6.3 kbar estimated for the veined migmatite. The magma veins propagated by means of fracturing (Burg and Vanderhaeghe, 1993) effectively introduced H_2O and heat to the upper part of the country rock and formed the leucosome veins. The aqueous fluid percolated, where it could easily pass (Weber and Barbey, 1986), and triggered a partial and incipient melting in the mesosome of the veined migmatite (Pattison and Harte, 1988). Although

it is out of the scope of this study, the stromatic metatexite, which is distributed north of the veined migmatite, might have been placed at the uppermost level among the members of GOBM.

The isobaric cooling (IBC) event, which followed, ceased to record $\sim 660^\circ C$ at the shallower level (veined migmatite: ~ 5.5 kbar), and $\sim 700^\circ C$ at the deeper level (diatexite; ~ 6.2 kbar). These dT/dP s in the veined migmatite and the diatexite indicate that they suffered from a similar IBC (Table. 12), and thus, their relative difference in depth is maintained after the CMT emplacement. In the EGMB, the IBC events from ~ 650 to $\sim 850^\circ C$ at around 5-6 kbar, were traced in the granulite suites of the Chilka Lake region (Sen et al. 1995) and Anakapalle (Dasgupta et al., 1994; Sanyal and Fukuoka, 1995; Sengupta et al., 1997). The P-T path for the Anakapalle area is interpreted as indicating that the crust with a normal thickness suffered from heat input by thinning lithospheric mantle, followed by crustal thinning and cooling (Dasgupta et al., 1994). In this model, the heat input to the crust by rift-related basalt is enough to initiate the melting (Sengupta et al., 1996). In the case of the Tekkali area, this may be applicable, although rock indicative of mafic intrusion concomitant with the CMT does not occur. It has been suggested that the CMT was raised from partial melting that was induced by Ti-rich mafic magma derived from the mantle (Chacko et al., 1996; Kilpatrick and Ellis, 1992). Zhao et al. (1997), however, recently showed an igneous charnockite, which was formed under a collisional setting. The tectonic setting of the Tekkali area needs further investigation.

Conclusions

The garnet-orthopyroxene-biotite migmatite (GOBM) around Tekkali changes its lithology from stromatic migmatite, veined migmatite to plutonic diatexite from north to south. The protolith of the GOBM is considered likely to be metagraywacke, as indicated by the occurrence and typical composition of garnet porphyroblast and Opx 1 as phases coexisting with the melt. Estimated pressure-temperature conditions indicate melting initiated at around $760^\circ C$ and 6.3 kbar under the effect of fluid (aqueous rather than carbonic). The heat and fluid input was from high temperature ($\sim 880^\circ C$) CMT emplacement at deeper levels (~ 7.5 kbar), the main body of which presently forms the diatexite. Retrograde garnet surrounding Opx 2 records an isobaric cooling event at $\sim 660^\circ C$ and 5.5 kbar for shallower, and $\sim 700^\circ C$ and ~ 6.2 kbar for deeper levels. The IBC event, which is consistent with the paths obtained from other localities of the EGMB, is considered to have followed a high-temperature CMT emplacement.

Acknowledgements

The author is deeply obliged to Prof. S. Yoshikura, Dr. Y. Osanai, Dr. Y. Yoshimura, Dr. T. Okudaira, Mr. D. Doyama and Mr. K. Nakaminami for their heartfelt assistance in analysis and discussion, to Prof. A.T. Rao for hospitality and discussion during author's stay in India, and to Prof. M. Yoshida for his encouragement during the study. Discussion and checking of the manuscript by Dr. H.M. Rajesh were the most appreciated. This work formed a part of author's Msc study and is partially supported by Grant-in-Aid, International Scientific Research of the Japan Ministry of Education, Science and Culture (MONBUSHO) for the 1997-1998 fund (No. 08041109), by UNESCO-IUGS-IGCP 368 and by the Gondwana Research Group.

References

- Abrecht, J. and Hewitt, D.A. (1988) Experimental evidence on the substitution of Ti in biotite. *Am. Mineral.*, **73**, 1275-1284.
- Abdel-Rahman, A.M. (1994) Nature of biotites from alkali-line, calc-alkaline, and peraluminous magmas. *Jour. Petrol.*, **35**, 525-541.
- Allibone, A.H. and Noriss, R.J. (1992) Segregation of leucogranite microplutons during syn-anatetic deformation: an example from the Taylor Valley, Antarctica. *Jour. Metamorphic Geol.*, **10**, 589-600.
- Aranovich, L.Y. and Newton, R.C. (1998) Reversed determination of the reaction: phlogopite + quartz = enstatite + potassium feldspar + H₂O in the ranges 750-875°C and 2-12 kbar at low H₂O activity with concentrated KCl solutions. *Am. Mineral.*, **83**, 193-204.
- Bence, A.E. and Albee, A.L. (1968) Empirical correction factors for the electron microanalysis of silicates and oxides. *Jour. Geol.*, **76**, 382-403.
- Bhattacharya, A., Krishnakumar, K.R., Raith, M. and Sen, S.K. (1991) An improved set of a-X paremeters for Fe-Mg-Ca garnets and refinements of the orthopyroxene-garnet thermometer and the orthopyroxene-garnet-plagioclase-quartz barometer. *Jour. Petrol.*, **32**, 629-656.
- Braun, I., Raith, M. and Ravindra Kumar, G.R. (1996) Dehydration-melting phenomena in leptynitic gneiss and the generation of leucogranites: a case study from the Kerala Khondalite Belt, southern India. *Jour. Petrol.*, **37**, 1285-1305.
- Burg, J.-P. and Vanderhaeghe, O. (1993) Structures and way-up criteria in migmatites, and its application to the Velay dome (French Massif Central). *Jour. Str. Geol.*, **15**, 1293-1301.
- Busch, W., Schneider, G. and Mehnert, K.R. (1974) Initial melting at grain boundaries, part II: melting in rocks of granodioritic to tonalitic composition. *Neu. Jahrb. Mineral. Monut.*, 345-370.
- Chacko, T., Lamb, M. and Farquhar, J. (1996) Ultra-high temperature metamorphism in the Kerala Khondalite Belt. *Gondwana Res. Gr. Mem.*, **3**, 157-165.
- Clemens, J.D. and Vielzeuf, D. (1987) Constraints on melting and magma production in the crust. *Earth Planet. Sci. Lett.*, **86**, 287-306.
- Conrad, W.K., Nicholls, I.A. and Wall, V.J. (1988) Water-saturated and -undersaturated melting of metaluminous and peraluminous crustal compositions at 10 kb: evidence for the origin of silicic magmas in the Taupo Volcanic Zone, Newzealand, and other occurrences. *Jour. Petrol.*, **29**, 765-803.
- Dasgupta, S., Sengupta, P., Fukuoka, M. and Chakraborti, S. (1992) Dehydration melting, fluid buffering and decompressional P-T path in a granulite complex from the Eastern Ghats, India. *Jour. Metamorphic Geol.*, **10**, 777-788.
- Dasgupta, S., Sanyal, S., Sengupta, P. and Fukuoka, M. (1994) Petrology of granulites from Anakapalle-evidence for Proterozoic decompression in the Eastern Ghats, India. *Jour. Petrol.*, **35**, 433-459.
- Dahl, O. (1969) Irregular distribution of iron and magnesium among coexisting biotite and garnet. *Lithos*, **2**, 311-322.
- Dymek, R.F. (1983) Titanium, aluminum and interlayer cation substitutions in biotite from high-grade gneisses, West Greenland. *Am. Mineral.*, **68**, 880-899.
- Farmer, G.L. and Boettcher, A.L. (1981) Petrologic and crystal-chemical significance of some deep-seated phlogopite. *Am. Mineral.*, **66**, 1154-1163.
- Fitzsimons, I.C.W. (1996) Metapelitic migmatites from Brattstrand Bluffs, East Antarctica-metamorphism, melting and exhumation of the mid crust. *Jour. Petrol.*, **37**, 395-414.
- Fitzsimons, I.C.W. and Harley, S.L. (1994) The influence of retrograde cation exchange on granulite P-T estimates and a convergence technique for the recovery of peak metamorphic conditions. *Jour. Petrol.*, **35**, 543-576.
- Ganguly, J., Cheng, W. and Tirone, M. (1996) Thermodynamics of aluminosilicate garnet solid solution: new experimental data, an optimized model, and themetric application. *Contrib. Mineral. Petrol.*, **126**, 137-151.
- Garrison, Jr., J.R. and Taylor, L.A. (1981) Petrogenesis of pyroxene-oxide intergrowths from kimberlite and cumulate rocks: co-precipitation or exsolution ? *Am. Mineral.*, **66**, 723-740.
- Green, T.H. (1977) Garnet in silicic liquids and its possible use as a P-T indicator. *Contrib. Mineral. Petrol.*, **65**, 59-67.

- Guidotti, C.V. (1984) Micas in metamorphic rocks. *Rev. Mineral.*, **13**, 357-467.
- Harley, S.L. (1984) An experimental study of the partitioning of Fe and Mg between garnet and orthopyroxene. *Contrib. Mineral. Petro.*, **86**, 359-373.
- Holtz, F. and Johannes, W. (1991) Genesis of peraluminous granites I. Experimental investigation of melt compositions at 3 and 5 kb and various H₂O activities. *Jour. Petro.*, **32**, 935-958.
- Johannes, W. (1989) Melting of plagioclase-quartz assemblages at 2 kbar water pressure. *Contrib. Mineral. Petro.*, **103**, 270-276.
- Jung, S., Mezger, K., Masberg, P., Hoffer, E. and Hoernes, S. (1998) Petrology of an intrusion-related high-grade migmatite: implications for partial melting of metasedimentary rocks and leucosome-forming processes. *Jour. Metamorphic Geol.*, **16**, 425-445.
- Kilpatrick, J.A. and Ellis, D.J. (1992) C-type magmas: igneous charnockites and their extrusive equivalents. *Trans. Royal Soc. Edinburgh Earth Sci.*, **83**, 155-164.
- Kretz, R. (1983) Symbols for rock-forming minerals. *Am. Mineral.*, **68**, 277-279.
- Lal, R.K. (1993) Internally consistent recalibrations of mineral equilibria for geothermobarometry involving garnet-orthopyroxene-plagioclase-quartz assemblages and their application to the South Indian granulites. *Jour. Metamorphic Geol.*, **11**, 855-866.
- Le Breton, N. and Thompson, A.B. (1988) Fluid-absent (dehydration) melting of biotite in metapelitic in the early stages of crustal anatexis. *Contrib. Mineral. Petro.*, **99**, 226-237.
- Lee, H.Y. and Ganguly, J. (1988) Equilibrium compositions of coexisting garnet and orthopyroxene: experimental determinations in the system FeO-MgO-Al₂O₃-SiO₂, and applications. *Jour. Petro.*, **29**, 93-113.
- Mazurek, M. (1992) Phase equilibria and oxygen isotopes in the evolution of metapelitic migmatites: a case study from the Pre-Alpine basement of Northern Switzerland. *Contrib. Mineral. Petro.*, **109**, 494-510.
- Montel, J.-M. and Vielzeuf, D. (1997) Partial melting of metagraywackes, part II. Compositions of minerals and melts. *Contrib. Mineral. Petro.*, **128**, 176-196.
- Morimoto, N., Fabries, J., Ferguson, A.K., Ginzberg, I.V., Ross, M., Seifert, F.A., Zussman, J., Aoki, K. and Gottardi, G. (1989) Nomenclature of pyroxenes. *Mineral. Mag.*, **52**, 535-550.
- Newton, R.C. (1992) An overview of charnockite. *Precamb. Res.*, **55**, 399-405.
- Newton, R.C. and Perkins III, D. (1983) Thermodynamic calibration of geobarometers based on the assemblages garnet-plagioclase-orthopyroxene (clinopyroxene)-quartz. *Am. Mineral.*, **67**, 203-222.
- Niimi, N. and Yamamoto, T. (1998) An inclusion in garnet porphyroblast in a granulite facies migmatite. *Abst. Ann. Meeting Mineral. Soc. Japan.* 133. (in Japanese)
- Osanai, Y., Owada, M., Shimura, T., Kawasaki, T. and Hensen, B.J. (1997) Crustal anatexis and related acidic magma genesis in the Hidaka metamorphic belt, Hokkaido, northern Japan. *Mem. Geol. Soc. Japan.*, **47**, 29-42. (Japanese with English abstract)
- Owen, J.V. and Greenough, J.D. (1997) Migmatites from Grenville, Quebec: metamorphic P-T-X conditions in transitional amphibolite/granulite-facies rocks. *Lithos*, **39**, 195-208.
- Owens, B.E. and Dymek, R.F. (1995) Significance of pyroxene megacrysts for massif anorthosite petrogenesis: constraints from the Labrieville, Quebec, pluton. *Am. Mineral.*, **80**, 144-161.
- Patiño Douce, A.E. and Beard, J.S. (1995) Dehydration-melting of biotite gneiss and quartz amphibolite from 3-15 kbar. *Jour. Petro.*, **36**, 707-738.
- Pattison, D.R.M. and Harte, B. (1988) Evolution of structurally contrasting anatexic migmatites in the 3-kbar Ballachulish aureole, Scotland. *Jour. Metamorphic Geol.*, **6**, 475-494.
- Robert, J.-L. (1976) Titanium solubility in synthetic phlogopite solid solutions. *Chem. Geol.*, **17**, 213-227.
- Rollinson, H. (1993) Using geochemical data: evaluation, presentation, interpretation. Longman. pp. 352.
- Sanyal, S. and Fukuoka, M. (1995) P-T-D history of granulites from Anakapalle, Eastern Ghats-evidence for polyphase (?) granulite metamorphism. *Mem. Geol. Soc. India.*, **34**, 125-141.
- Sen, S.K. and Bhattacharya, S. (1984) An orthopyroxene-garnet thermometer and its application to the Madras charnockite. *Contrib. Mineral. Petro.*, **88**, 64-71.
- Sen, S.K., Bhattacharya, S. and Acharyya, A. (1995) A multi-stage pressure-temperature record in the Chilka lake granulites: the epitome of the metamorphic evolution of Eastern Ghats, India? *Jour. Metamorphic Geol.*, **13**, 287-298.
- Sengupta, P., Dasgupta, S., Bhui, U.K., Ehl, J. and Fukuoka, M. (1996) Magmatic evolution of mafic granulites from Anakapalle, Eastern Ghats, India: implications for tectonic setting of a Precambrian high-grade terrain. *Jour. Southeast Asia. Earth Sci.*, **14**, 185-198.
- Sengupta, P., Sanyal, S., Dasgupta, S., Fukuoka, M., Ehl, J. and Pal, S. (1997) Controls of mineral reactions in high-grade garnet-wollastonite-scapolite-bearing calcsilicate rocks: an example from Anakapalle, Eastern Ghats, India. *Jour. Metamorphic Geol.*, **15**, 551-564.
- Singh, J. and Johannes, W. (1996a) Dehydration melting of

- tonalites. Part I. Beginning of melting. *Contrib. Mineral. Petrol.*, **125**, 16-25.
- Singh, J. and Johannes, W. (1996b) Dehydration melting of tonalites. Part II. Composition of melts and solids. *Contrib. Mineral. Petrol.*, **125**, 26-44.
- Skjerlie, K.P. and Johnston, A.D. (1993) Fluid-absent melting behavior of an F-rich tonalitic gneiss at mid-crustal processes: implications for the generation of anorogenic granite. *Jour. Petrol.*, **34**, 785-815.
- Stevens, G., Clemens, J.D. and Droop, G.T.R. (1997) Melt production during granulite-facies anatexis: experimental data from "primitive" metasedimentary protolith. *Contrib. Mineral. Petrol.*, **128**, 352-370.
- Vielzeuf, D. and Montel, J.-M. (1994) Partial melting of metagreywackes. part I. fluid-absent experiments and phase relationships. *Contrib. Mineral. Petrol.*, **117**, 375-393.
- Watson, E.B. and Harrison, T.M. (1983) Zircon saturation revisited: temperature and composition effects in a variety of crustal magma types. *Earth Planet. Sci. Lett.*, **64**, 295-304.
- Weber, C. and Barbey, P. (1986) The role of water, mixing processes and metamorphic fabric in the genesis of the Baume migmatites (Ardèche, France). *Contrib. Mineral. Petrol.*, **92**, 481-491.
- Whalen, J.B., Currie, K.L. and Chappell, B.W. (1987) A-type granites: geochemical characteristics, discrimination and petrogenesis. *Contrib. Mineral. Petrol.*, **95**, 407-419.
- Wickam, S.M. (1987) Crustal anatexis and granite petrogenesis during low-pressure regional metamorphism: the Trois Seigneure Massif, Pyrenees, France. *Jour. Petrol.*, **28**, 127-169.
- Yamamoto, T., Tani, Y., Miyashita, Y., Rao, A.T. and Yoshida, M. (1998) Migmatite and granulites in the Patapatnam-Tekkali area, Eastern Ghats, India. *Jour. Geosci. Osaka City Univ.*, **41**, 123-142.
- Zhao, J.-X., Ellis, D.J., Kilpatrick, J.A. and McCulloch, M.T. (1997) Geochemical and Sr-Nd isotopic study of charnockite and related rocks in the northern Prince Charles Mountains, East Antarctica: implications for charnockite petrogenesis and proterozoic crustal evolution. *Precamb. Res.*, **81**, 37-66.

Manuscript received November 5, 1998.

Revised manuscript accepted March 8, 1999.